

1 **The origin of the Gravettians: genomic evidence from a 36,000-year-old Eastern**
2 **European**
3

4 E. Andrew Bennett¹, Sandrine Prat², Stéphane Péan³, Laurent Crépin³, Alexandr Yanevich⁴,
5 Simon Puaud², Thierry Grange¹, Eva-Maria Geigl¹

6

7 ¹Institut Jacques Monod, CNRS, Université de Paris, 75013 Paris, France; ²UMR 7194 (HNHP),
8 MNHN/CNRS/UPVD, Alliance Sorbonne Université, Musée de l'Homme, Palais de Chaillot, 17
9 Place du Trocadéro, 75116, Paris, France; ³UMR 7194 (HNHP), MNHN/CNRS/UPVD, Muséum
10 national d'Histoire naturelle, Alliance Sorbonne Université, Institut de Paléontologie Humaine, 1
11 rue René Panhard, 75013, Paris, France; ⁴Institute of Archaeology, National Academy of Sciences
12 of Ukraine, Heroiv Stalingrada 12, 04210 Kyiv, Ukraine.

13

14

15

16

17

18

19

20

21 **Abstract**

22 **The Gravettian technocomplex was present in Europe from more than 30,000 years ago until**
23 **the Last Glacial Maximum, but the source of this industry and the people who manufactured**
24 **it remain unsettled. We use genome-wide analysis of a ~36,000-year-old Eastern European**
25 **individual (BuranKaya3A) from Buran-Kaya III in Crimea, the earliest documented**
26 **occurrence of the Gravettian, to investigate relationships between population structures of**
27 **Upper Palaeolithic Europe and the origin and spread of the culture. We show BuranKaya3A**
28 **to be genetically close to both contemporary occupants of the Eastern European plain and**
29 **the producers of the classical Gravettian of Central Europe 6,000 years later. These results**
30 **support an Eastern European origin of an Early Gravettian industry practiced by members**
31 **of a distinct population, who contributed ancestry to individuals from much later Gravettian**
32 **sites to the west.**

33

34

35

36

37

38

39

40

41

42 **Introduction**

43 Since the 19th century, archaeologists have defined similarities identified across material remains
44 as an archaeological culture, complex, or in some cases, a “people”, and used these definitions to
45 trace the mobility, interactions, and technical development of past populations. The burgeoning
46 field of ancient DNA analysis allows past populations to be studied directly, and the genetic
47 relationships of the manufacturers of materially defined cultures can now be characterized. While
48 palaeogenomics and archaeological culture describe two separate past phenomena, they are not
49 always unrelated, and Upper Palaeolithic (UP) Europe has shown surprising correlations between
50 closely-related genetic clusters and archeologically defined material industries¹. The Gravettian
51 technocomplex defines European Mid-Upper Palaeolithic (MUP) industries characterized by a
52 suite of shared innovations, along with specific modalities of their production, such as stone
53 Gravette points, backed blades and bladelets, personal ivory and shell ornaments, ochre, and antler
54 or bone tools. The Gravettian became widespread throughout Europe beginning after ca. 36,000²
55 until ca. 23,000³ cal BP years ago (ca. 32-21 ka ¹⁴C BP). The technocomplex defined by this term,
56 however, is by no means homogeneous, describing rather shared practices across many regional
57 *facies* and evolving *stages*³ (See Supplementary Text). While the Gravettian is considered to be a
58 local European industry, its origins continue to be the subject of ongoing research and debate⁴. The
59 density of Gravettian sites found in the Danubian valley radiocarbon dated as early as ca. 36,000
60 years cal BP have been used to argue for a local evolution of the Gravettian from the technical
61 legacy of the Aurignacian in the upper valley⁵, or through acculturation with post-Mousterian leaf-
62 point transition industries, such as the Szeletian, in the Middle Danubian basin⁶. However, long-
63 recognized similarities between features of Gravettian lithic traditions and Near Eastern industries,
64 such as the Ahmarian, which is found 10,000 years earlier in the Levant, as well as similar Early-

65 Upper Palaeolithic (EUP) micro-laminar industries found in both northern and southern slopes of
66 the Caucasus suggest an earlier influence from the southeast⁷⁻⁹.

67 Although the integration of Eastern European EUP and MUP traditions into an archaeological
68 framework defined in Central and Western Europe has historically been problematic, recent
69 reassessments of EUP assemblages from the Caucasus¹⁰⁻¹² emphasize similar lithic traditions
70 among roughly contemporaneous (40-30,000 cal BP) layers at sites such as Dzudzuana Cave (layer
71 D), Ortvale Klde (layer 4c), Mezmaiskaya Cave (layer 1C), and the six layers of Buran Kaya III
72 (layer 6-5 to 5-2) in Crimea^{13,14} (see Supplementary Text for the stratigraphy of Buran-Kaya III).
73 Some authors suppose that the appearance of these Caucasian and Eastern European EUP
74 assemblages, which include backed blades and bladelets, are primarily based on the distribution
75 and transformation of Ahmarian traditions from Near East to Europe, probably through the
76 Caucasus, independent of that which brought the proto-Aurignacian to Central and Southern
77 Europe and the Mediterranean area^{10,14-16}. The parallels between these Eastern European industries
78 and the Gravettian appearing later in Central Europe and the Danubian Valley have led some to
79 propose the term “Early Gravettian” to describe these industries to distinguish them from the
80 classical Gravettian^{8,16,17}. However, the relationship of this Early Gravettian identified in Eastern
81 Europe to the development of the Gravettian in the west, as well as the extent to which it may have
82 involved transfers and adaptations of technology and movements of people, are unclear. The direct
83 study of the populations associated with these industries through genomic analysis of skeletal
84 remains from key archaeological sites will likely clarify this process and answer important
85 questions concerning how technologies disperse and change in UP societies.

86 Several human remains associated with the classical Gravettian from Central Europe, Belgium and
87 Italy were previously analysed genetically and found to share more genetic drift with each other

88 than individuals associated with other material cultures¹. This group was termed the *Vestonice*
89 *cluster*, after Vestonice16, the best-covered genome from the ca. 30,000-year-old (cal BP)
90 Gravettian site Dolní Věstonice II in the Czech Republic. Interestingly, Vestonice16 and other
91 high-coverage genomes from the Gravettian sites Krems-Wachtberg (Austria) and Ostuni (Italy)
92 have been found to be admixed, deriving between 40 to 90% of their ancestry from a lineage
93 related to Kostenki14^{1,18}, an individual living ca. 7,000 years earlier at the Kostenki-14 site found
94 in the Borshchovo archaeological complex of Western Russia, linking Gravettians of Central
95 Europe and the Apennine peninsula with an earlier population farther east.

96 While the Kostenki14 burial has no associated cultural material, contemporaneous Gravettian
97 artefacts have been recovered in Eastern Europe from three cultural layers at Buran-Kaya III in
98 Crimea and dated between ca. 38-34,000 cal BP^{2,19}. Discovered in 1990, the Buran-Kaya III rock
99 shelter contains stratigraphic layers spanning from the Middle Palaeolithic to the Middle Ages.
100 The Gravettian layers have yielded backed microliths, microgravette points, ochre, body
101 ornaments of ivory, shell, and teeth, as well as multiple human skull fragments showing signs of
102 post-mortem processing². Buran-Kaya III is the earliest site bearing Gravettian material²⁰ (see
103 Supplementary Text), yet it remains a distant outlier, both geographically and temporally, to the
104 more densely clustered appearances of the Gravettian occurring several thousand years later and
105 2,000 km to the west in the Danubian valley and the Swabian Jura, such as Krems-Hundssteig and
106 Geißenklösterle, respectively.

107 To genetically characterize one of the earliest manufacturers of the Gravettian complex and how
108 they relate to other known MUP populations, as well as to further explore the relationships between
109 UP populations and the material culture they made, we present genome-wide data from a human
110 parietal bone fragment, BuranKaya3A, aseptically excavated in 2009 from layer 6-1 of Buran-

111 Kaya III (see Supplementary Text). Radiocarbon (AMS) dates from a different human cranial
112 fragment from this layer range from 36,260 to 35,280 cal BP (31,900+210-220 ^{14}C BP)² (Figure 1
113 and Table S1), which is located between two other Gravettian layers, while all dated material (n=4)
114 from the same layer ranges from 37,560-33,850 cal BP¹⁹.

115

116 **Results**

117

118 Initial genetic characterization of BuranKaya3A revealed extremely poor preservation of
119 endogenous DNA, both in fragment length and in low quantity relative to environmental DNA,
120 but little contamination with modern human DNA as assessed by quantitative PCR. In order to
121 identify the most efficient material for mitochondrial enrichment and shotgun genome sequencing,
122 our strategy was to 1) screen single-stranded DNA libraries by both shallow shotgun sequencing
123 and mitochondrial enrichment from eight extractions taken from four different areas of the sample
124 and subjected to two different extraction treatments, 2) identify the extract that performed best in
125 terms of highest sequence complexity, endogenous content, and lowest modern human
126 contamination, and 3) construct a second series of single-stranded libraries with and without UNG
127 for deeper mitochondrial enrichment and shotgun sequencing. The best candidate identified from
128 the screening results contained 0.34% endogenous DNA (see *Methods* section and Extended Data
129 Figure 1). The second series of libraries from this extract was used to generate 82-fold coverage
130 of the mitochondrial genome and shotgun nuclear data (Table S2).

131

132

133 **Mitochondrial and Y-chromosome haplogroups**

134 The mitochondrial haplogroup of BuranKaya3A was determined to belong to an early branch of
135 the N lineage, N1. Surprisingly, this assignment falls outside of the lineages previously reported
136 for UP Europe, nearly all of which derive from later N branches (U and R haplogroups, Figure 2).
137 The N1 of BuranKaya3A is notably distinct from the mitochondrial haplogroup N identified from
138 the roughly 40,000-year-old mandible from Peștera cu Oase in Romania, which belongs to a more
139 basal branch that has no modern descendants²¹. In addition, the N1 of BuranKaya3A carries three
140 of the eight mutations occurring prior to N1b, a rare haplogroup most highly concentrated in the
141 Near East, yet appearing broadly from western Eurasia to Africa. The descendants of the N1b node
142 include N1b2, currently found only in Somalia²², and N1b1b, found in nearly 10% of Ashkenazi
143 Jewish haplogroups²³. These three mutations allow us to place BuranKaya3A on a lineage apart
144 from that which has been proposed to later enter Europe from Anatolia during the Neolithic
145 (N1a1a)²⁴. Among ancient samples, the mitochondrial sequence of an 11,000-year-old
146 Epipalaeolithic Natufian from the Levant (“Natufian9”)²⁵ is also a later derivative of this N1b
147 branch. Thus, mitochondrial sequences branching both upstream and downstream of the
148 BuranKaya3A sequence can be traced to the Near East, and the modern presence in Europe of
149 haplogroups descended from the N1 (N1b1b and N1a1a) branch to which BuranKaya3A belongs
150 appear to be due to later migrations from the Near East (Extended Data Figure 2). We determined
151 the genetic sex of BuranKaya3A to be male using both the ratio of chromosome X and Y mapped
152 reads, giving an R_y value of 0.0893-0.097 (95% CI, SE 0.002)²⁶, as well as a ratio of chromosome
153 X mapped reads to the average of autosomal reads of 0.55 (a ratio near 1.0 would indicate diploid
154 for X). From the reads mapping to the Y chromosome, six out of six Single Nucleotide
155 Polymorphisms (SNPs) that overlap with diagnostic sites for Y-haplogroup BT all carry the

156 derived allele, allowing a minimum assignment to BT, which has origins in Africa, with additional
157 derived alleles suggesting an eventual placement of CT or C, found in Asia and the Epipalaeolithic
158 Near East²⁵. Additional ancestral alleles make an assignment of C1a2 or C1b, which appear in UP
159 Europe¹, unlikely (see Table S3 for a summary and comparative placement of Palaeolithic Y-
160 haplogroups, and Supplementary Data 1 for a complete list of Y diagnostic SNPs).

161

162 **Neanderthal ancestry**

163 Neanderthal settlements, attributed to the Micoquian, KiiK-Koba type, at Buran-Kaya III (layer B)
164 has been dated by faunal bone fragments to 43.5 to 39.6 ka cal BP¹⁹, demonstrating an earlier
165 Neanderthal presence at the site just prior to the Campanian Ignimbrite eruption (39,280±110 years
166 cal BP (⁴⁰Ar/³⁹Ar))²⁷. Anatomically Modern Human (AMH) remains dating to this period in
167 Romania have documented local admixture with late Neanderthals in Eastern Europe²¹, leading us
168 to investigate whether admixture with local Neanderthals in Crimea could be detected in early
169 AMHs living ca. 4,000 years after the presumed disappearance of Neanderthals from the
170 region^{19,28}. Neanderthal ancestry calculated using ancestry informative SNPs¹ on libraries from
171 four independent preparations determined that BuranKaya3A possesses 3.4% (SD 0.008)
172 Neanderthal ancestry (Table S4). This level of Neanderthal ancestry is typical for
173 contemporaneous West Eurasians and shows no evidence of late, local Neanderthal admixture in
174 Crimea with AMHs ancestral to the population to which BuranKaya3A belonged.

175

176 **Genomic relationships of UP Europe and their archaeological cultures**

177 The genetic relationship between BuranKaya3A and other UP individuals for which sufficient
178 genomic data exist can be measured using outgroup $f3$ -statistics and various D-statistical tests²⁹.
179 These were performed using SNPs from 52 previously published individuals dating from the Initial
180 Upper Palaeolithic (IUP) to the Mesolithic that had been reprocessed in the same pipeline used for
181 BuranKaya3A to reduce possible artefacts that may arise from data coming from disparate sources.
182 27,774 SNPs having base quality 30 or above were identified in BuranKaya3A that overlapped
183 with the nearly 3M SNPs from the combined panels in Fu *et al.* 2016¹. To minimize standard
184 errors, we restricted the results of this analysis to include only individuals having more than
185 300,000 SNPs overlapping with the panel.

186 Outgroup $f3$ -statistics quantify the amount of shared genetic drift between two populations relative
187 to an outgroup population and have been used to reveal genetic affinities among UP individuals¹.
188 Of the 21 ancient individuals (x) including at least 1000 SNPs in the calculation: $f3(\text{BuranKaya3A},$
189 $x; \text{Mbuti})$ or $f3(\text{BuranKaya3A}, x; \text{Han})$, the highest $f3$ values for both outgroups were found when
190 x was either Sunghir3 (SIII), a 34,000-year-old (cal BP) group burial characterized as either
191 Streletsian³⁰ or Eastern Gravettian^{31,32} (see Supplementary Text) found ca. 1,300 km to the
192 northeast of Buran-Kaya III, Vestonice16, from the context of a Gravettian *facies* known as the
193 Pavlovian, who lived ca. 6,000 years later and ca. 1,400 km to the northwest, and Kostenki14, a
194 burial predating BuranKaya3A by ca. 1,000 years and lying ca. 1,100 km to the northeast (Figure
195 3). Notably, BuranKaya3A shows less affinity for the 35,000-year-old (cal BP) GoyetQ116-1 from
196 Goyet cave in Belgium, with no direct cultural association, but dated to the Aurignacian period in
197 this area^{1,33}, as well as the El Miron cluster, which corresponds to European late glacial
198 (Magdalenian) hunter-gatherers¹. BuranKaya3A was also found to be particularly distant from the
199 Villabruna cluster, representing European post-glacial hunter-gatherers (Figure 3 and Extended

200 Data Figure 3A-B). The individual from Buran-Kaya III can thus be defined as a member of a
201 population making an Early Gravettian in Eastern Europe whose closest known genetic
202 relationships are with populations living within a 3,000-year window (ca. 37,000-34,000 cal BP)
203 farther northeast on the Eastern European plains (Sunghir3 and Kostenki14), as well as with
204 Gravettian populations who appeared ca. 6,000 years later in Central Europe (Vestonice16).

205 We then applied D-statistics to measure shared drift between BuranKaya3A and the individuals
206 tested above (x) as compared to the 45,000-year-old (cal BP) Central Asian Ust-Ishim ($D(x, Ust-$
207 Ishim; BuranKaya3A, Mbuti)), shown to be basal to all western MUP Eurasians studied to date³⁴
208 (Figure 4a). Substituting the modern Han for Ust-Ishim gives additional support for the above
209 relationships with greater significance (Z-scores > 2.5) (Figure 4b). Full results for all tested
210 samples using both all SNPs and transversions only are given in Extended Data Figures 4 and 5.
211 The D-statistics support the results of the outgroup $f3$ -statistical tests, except that here Sunghir3 is
212 replaced by Vestonice16 as sharing the most alleles with BuranKaya3A, although we note results
213 from both Vestonice16 and Sunghir3 overlap within one standard error. The additional D-statistic
214 $D(w, x; BuranKaya3A, Mbuti)$, where w and x are various well-covered ancient individuals
215 representing previously defined Eurasian populations, was unable to significantly resolve which
216 of these two individuals is most closely related genetically to BuranKaya3A: the ca. 34,000-year-
217 old (cal BP) East European Sunghir3 or the ca. 30,000-year-old (cal BP) Central European
218 Vestonice16 (Extended Data Figure 6).

219 Genomic data from less well covered MUP Europeans allows us to better define the relative
220 position of BuranKaya3A with more individuals from Gravettian contexts, including
221 representatives of two of the three previously identified *Vestonice* genetic sub-clusters
222 corresponding to Gravettian sites¹. Comparing two low-coverage individuals requires more

223 caution in interpreting the results due to the low number of SNPs used for the calculations.

224 However, we were able to establish additional support for the relationships by applying a strict

225 filtering process whereby 1) we performed the analysis using two datasets, one including all SNPs

226 and the other considering only the transversions. The transversion-only dataset reduces the number

227 of SNPs used, but eliminates statistical noise from deaminated cytosines, a common form of

228 damage in ancient DNA. 2) We excluded samples using less than 50 SNPs for $f3$ analysis in the

229 smaller transversion-only dataset. 3) We required the resulting values from both datasets to be

230 within 30% of each other. This approach allowed us to define genetic affinities between

231 BuranKaya3A and the following individuals: Kostenki12, a 32,500-year-old (cal BP) neonate

232 whose remains were found at the Kostenki-Borshchovo archaeological complex in Russia and

233 associated with a cultural layer attributed to a local industry defined as the Gorodtsovian³⁵;

234 Vestonice43 and Pavlov1, two Central European Gravettian (Pavlovian) burials similar in age and

235 location to Vestonice16 and belonging to the “Vestonice Central European” genetic subcluster;

236 Paglicci133, a ca. 33,000-year-old (cal BP) tooth from the Apulia region of Southern Italy found

237 in association with Early Gravettian cultural material; and Ostuni1, a ca. 27,500 year-old (cal BP)

238 Gravettian burial, also from the Apulia region and both belonging to the “Vestonice Italian”

239 genetic subcluster. No members of the “Vestonice Goyet” subcluster from Goyet cave in Belgium

240 passed our filters to be included in the analysis (full descriptions of these samples and clusters are

241 given in the Supplementary Information of Fu et al. 2015¹). Visual representation of the outgroup

242 $f3$ -statistics, $f3$ (BuranKaya3A, *MUP*; *Mbuti*), for all samples passing filters is shown in Extended

243 Data Figure 7 and full results for all tested samples are given in Extended Data Figure 8.

244 Of the less well-covered samples, Kostenki12 is shown to have a high affinity with BuranKaya3A.

245 This is in agreement with the previously reported affinity between Kostenki12 and Sunghir3³⁶ and

246 closely links BuranKaya3A to all EUP and MUP individuals currently known from the Eastern
247 European plains. To the west, BuranKaya3A shows close genetic affinity with Pavlov1, followed
248 more distantly by Vestonice43 and Ostuni1, and at a greater distance, the older Paglicci133. In
249 summary, these results allow us to firmly establish a close genetic relationship between
250 BuranKaya3A with contemporary EUP and MUP populations of the Eastern European plains, as
251 well as the broader population manufacturing the Pavlovian *facies* of the Gravettian in Central
252 Europe ca. 6,000 years later, but less so with those associated with the Gravettian of southern Italy.
253 This implies a network of gene flow across the Eastern European plains and the Danubian Valley
254 between 37,000-30,000 years ago (cal BP) which, apart from the local Gorodtsovian culture found
255 at Kostenki 12, can be associated with various *facies* of the Gravettian technocomplex. The results
256 from Ostuni1 and Paglicci133 indicate a more indirect relationship between these populations and
257 BuranKaya3A. Higher coverage genetic information from early Gravettian sites in Italy will be
258 required to better understand to what extent the movements of people and ideas lead to the
259 appearance of the Gravettian in the southern Apennine Peninsula.

260

261 **Low Common West Eurasian ancestry in UP Eastern Europe**

262 Ancestry from a population which split from all non-Africans prior to their separation from each
263 other, termed Basal Eurasian, had not been known in Europe until after the Last Glacial Maximum
264 (LGM)¹. However, two 24,000-27,000-year-old (cal BP) individuals from layer C at Dzudzuana
265 Cave in the southern Caucasus have recently been reported to share ~70% common ancestry with
266 Villabruna and ~30% ancestry deriving from this Basal-Eurasian source¹⁸. Additionally, varying
267 layers of Villabruna ancestry, which did not enter Europe in an unmixed form prior to ca. 14,000
268 years ago (cal BP)¹, have been found in members of the Gravettian Vestonice cluster as well as

269 the Magdalenian El Miron cluster, indicating a degree of shared ancestry in these groups with a
270 “Common West Eurasian” population¹⁸. We calculated the relative level of Basal Eurasian
271 ancestry using D-statistic $D(EUP\ East\ Asian, UP, \text{Ust-Ishim, Mbuti})$, where a positive value
272 indicates Basal Eurasian ancestry as allele sharing between the UP individual and Africans. This
273 analysis showed BuranKaya3A, like other pre-LGM UP Europeans, to be lacking Basal Eurasian
274 ancestry (Extended Data Figure 9). Similar tests examine the relative affinities of Palaeolithic and
275 Mesolithic populations to Villabruna as opposed to either modern East Asians, $D(x, \text{Han; Villabruna, Mbuti})$, or BuranKaya3A, $D(x, \text{BuranKaya3A; Villabruna, Mbuti})$ (Extended Data
276 Figures 10 and 11, respectively). These results show levels of Villabruna ancestry in Eastern
277 European EUP individuals (Sunghir3, Kostenki12, Kostenki14, and BuranKaya3A) below that of
278 later UP Central and Western Europeans from Gravettian contexts (the Vestonice cluster).
279 Intriguingly, this includes a proportion of shared ancestry with Villabruna in BuranKaya3A similar
280 to that found in Ust-Ishim and both ancient and modern East Asians (Extended Data Figures 10
281 and 11), which should be insignificant based on previous admixturegraph analysis¹⁸.

283

284 **Discussion**

285

286 The results of the genome-wide analysis of BuranKaya3A offer important evidence linking the
287 previously established genetic signature of the manufacturers of the Gravettian in Central Europe
288 to a much earlier appearance of the Gravettian in Eastern Europe. The absence of the “Common
289 West Eurasian” ancestry, as represented by Villabruna, in BuranKaya3A marks a key genetic
290 distinction between the Gravettian inhabitants of Buran-Kaya III, possibly including the broader

291 populations of EUP Eastern Europe as well, and the UP populations of Western and Central
292 Europe, which is characterized by a West-to-East reduction in “Common West Eurasian” ancestry
293 (seen in Extended Data Figure 10). The association we show here of this eastern genetic character
294 with the cultural material of the Gravettian of Buran-Kaya III, which has been compared to nearby
295 contemporaneous Early Upper Palaeolithic assemblages from the Caucasus^{11,15} indicated in Figure
296 3, collectively support an eastern advance of AMHs during the EUP into Europe through the
297 Caucasus as has been previously proposed based on archaeological evidence alone^{7,8,16}. Such a
298 population would have had to have split from the settlers of Central Europe and the Mediterranean
299 prior to their acquisition of the Common West Eurasian component as represented by Villabruna.
300 In this scenario, the technical adaptations required for the challenging environment of the open
301 Eastern European plains, a dryer landscape with little natural shelter, as well as possible cultural
302 exchanges with local populations, may have played a role in the development of the Early
303 Gravettian industry⁸. The individuals recently characterized genetically from layer C of
304 Dzudzuana cave in the Caucasus (data not yet available), who were found to contain ancestry (both
305 Basal Eurasian and Common West Eurasian) that was absent ca. 9,000 years earlier in Crimea,
306 may represent more recent immigration into Eastern Europe. A higher resolution of these
307 movements awaits genetic analysis of more EUP and MUP sites from this region.

308 Numerous parallels in lithic industries, such as microblade-knapping methods, backed blades, and
309 analogous stone blade, point and tool morphology (such as the partly backed Ahmarian el Wad-
310 points and Gravette points of Europe) have suggested earlier Near Eastern cultures as possible
311 precursors to Gravettian techniques^{7,8}. Despite both uni-parental markers being shared between
312 BuranKaya3A and Epipalaeolithic Natufians in the Near East, we were unable to detect extensive
313 genome-wide allele-sharing between BuranKaya3A and the Natufians in our analysis. We note,

314 however, that the high level of Basal Eurasian ancestry in Natufian genomic sequences (38-54%²⁵)
315 limits our sensitivity when comparing populations lacking this component. For example, negative
316 D-statistics seen in Figure 4 involving the Mesolithic Caucasus Hunter-Gatherer (CHG)
317 individuals Kotias and Satsurblia³⁷, as well as the Natufians and the Iranian Hotu²⁵, are due to the
318 Basal Eurasian content reported for these individuals, which appears in the statistic as an affinity
319 toward the outgroup Mbuti. Also, given the more than 20,000-year age difference between
320 BuranKaya3A and the Natufians, it is unlikely that the Epipalaeolithic Natufians are the best
321 surrogates for EUP Near Eastern populations. While influences from the Ahmorian can be seen in
322 the Gravettian¹⁷, it is the Early Ahmorian that has separately been proposed as a source for the
323 wave of AMHs bringing the Proto-Aurignacian west, possibly by way of the Balkans, into Central
324 and Southern Europe beginning prior to the Campanian Ignimbrite eruption¹³. Populations
325 associated with the Early Ahmorian and the Ahmorian may thus suggest better candidate source
326 populations to investigate further the hypothesis of a population split behind separate routes in the
327 settling of Europe, the Balkans/Mediterranean to the west and the Caucasus to the east, each
328 associated with accompanying industries (Proto-Aurignacian and Early Gravettian, respectively).

329 The shared ancestry, as well as cultural similarities, demonstrated between the settlements at
330 Buran-Kaya III, later Gravettians in Central Europe, and to some extent, Sunghir, suggest a broad
331 and long-lasting network of social exchange in the EUP across Eastern and Central Europe, from
332 the Eastern European plains to the Danubian corridor. Given this background, the appearance of
333 the Gravettian in Central Europe in the MUP, where it later would blossom, is likely to have
334 resulted from this input from the east. While we show that the Gravettian, *sensu lato*, was not
335 practiced by a single genetically uniform cluster across all *facies*, the close genetic relationship
336 between BuranKaya3A and the Kostenki individuals raise further questions as to the origin of the

337 local culture termed Gorodtsovian, which is found at Kostenki 12 and unknown outside the
338 Kostenki-Borshchevo region. Given the genetic affinities we report, the previous assignment by
339 some authors of the Late Streletskian industry of Sunghir being a local *facies* of an “Eastern”
340 Gravettian^{31,32} should lead to a closer examination of the possible influences underlying the
341 appearance of the Gorodtsovian, with appreciation for the impact that climate, the specific
342 landscape of the site, and site-specific activities may have had on the individual tool requirements
343 of the assemblages⁸. Alternatively, the Gorodtsovian and other local UP industries of Eastern
344 Europe may represent distinct cultures practiced on the Eastern European plains, and the genomic
345 affinities between the individuals from Kostenki, Sunghir and BuranKaya3A may show only a
346 relationship to a common source population among the occupants of Eastern Europe branching
347 more recently than those present in Western Europe.

348 This study, the genomic analysis of the oldest AMH from an archeologically defined context,
349 demonstrates an underlying genetic continuity between manufacturers of various *facies* of the
350 Gravettian spanning ca. 9,000 years. A geographical divergence among groups entering Europe
351 more than 37,000 years ago is supported by the finding that the earliest appearance at Buran-Kaya
352 III is associated with a population unadmixed with the Common West Eurasian component already
353 present in Europe to some degree, and is thus distinct. Regional features such as micro-laminar
354 industries and Gravette points found in EUP assemblages in the Caucasus, both archeologically
355 comparable and contemporary with Buran-Kaya III, suggest the Caucasus as a possible route for
356 this diffusion, and a role of these industries in the development of the Early Gravettian. A more
357 comprehensive understanding of both genomic information and archaeological assemblages of UP
358 sites in the Caucasus and Near East will allow more precise identification of the origins of both
359 this population and, potentially, the Gravettian.

360 **Methods**

361

362 **Dating**

363 All radiocarbon dates were recalibrated using the software OxCal v4.3.2 based on the IntCal13
364 calibration data set³⁸. The calibrated dates are rounded to 5.

365 **Sample handling, DNA extraction, library construction, and sequencing**

366 A human parietal fragment was excavated aseptically from layer 6-1 during the 2009 excavation
367 season at Buran Kaya III (see Supplementary Text). All pre-amplification sample preparation was
368 performed in the dedicated ancient DNA facility using decontamination and clean-room protocols
369 as described in Bennett, et al³⁹. All buffers and solutions were prepared using water
370 decontaminated by gamma-irradiation (8 kGy). After first removing the surface of the areas to be
371 sampled with a sterile scalpel, between 47 and 114 mg of bone powder was recovered from four
372 different places of the bone using a variable-speed drill at low speed to reduce overheating
373 (Dremel, Mount Prospect, IL, USA). Two of these samplings were each divided into two equal
374 portions, one of which was subject to phosphate buffer pre-treatment as described in Korlevic, *et*
375 *al*⁴⁰. Phosphate buffer washes for each sample were collected and combined for DNA purification.
376 Both phosphate and non-phosphate buffer treated samples, including reagent-only mocks, were
377 then incubated in 1.5 mL LoBind microcentrifuge tubes (Eppendorf, Hamburg, Germany) with 1
378 mL 0.5 M EDTA , pH 8.0 (Sigma-Aldrich, St. Louis, MO), with 0.25mg/mL proteinase K (Sigma-
379 Aldrich) and 0.05% UV-irradiated Tween-20 (Sigma-Aldrich), at 37°C for 24 H. Following
380 incubation, all tubes were centrifuged at maximum speed for 10 min, and supernatant was mixed
381 with 10 times its volume of “2M70” binding buffer (2 M guanidine hydrochloride and 70%

382 isopropanol) in a 15 mL tube and passed through QIAquick silica columns (Qiagen, Hilden,
383 Germany) using 25 mL tube extenders (Qiagen) and a vacuum manifold (Qiagen) as described^{39,41}.
384 2M70 binding buffer has been shown to retain the smaller DNA fragments lost during purification
385 with traditional binding buffers⁴². Columns were washed twice with 1 mL PE Buffer (Qiagen) then
386 transferred to a micro-centrifuge and dried by spinning 1 minute at 16,100 × g, turning tubes 180°
387 and repeating. DNA was eluted in a total of 60 µl of 10 mM EBT (Tris-HCl pH 8.0 containing
388 0.05% Tween-20) performed in two elutions of 30 µl each, by spinning 16,100 × g for 1 minute
389 after a 5-minute incubation.

390 For the screening step, single-stranded libraries were constructed using either 2 µl (for screening)
391 or 6 µl (for mitochondrial capture) of the eluted DNA, including mocks of all treatments, water
392 only samples, and a positive control oligo following the protocol of Gansauge, *et al.*⁴³ using the
393 splinter oligonucleotide TL110, and eluting in 50 µl EBT. Either 40 µl (for mitochondrial capture)
394 or 4 µl (for screening) of each library was used for bar-coding amplification using dual-barcoded
395 single-stranded library adapters⁴⁴ as primers in the following 100 µl volume reaction: 10 µl 10x
396 PCR Buffer + MgCl2 (Roche, Basel, Switzerland) 0.4 µM of each primer, 80 µM dNTPs (Roche),
397 15 units of FastStart Taq (Roche). Reactions were heated 95°C for 5 min, followed by 35 cycles
398 of 95°C 20 s, 53°C for 45 s, 68°C for 45 s, and then 68°C for 5 min. Heteroduplexes that could
399 confound size selection were resolved by diluting the PCR product 1:5 in a 100 µl reaction
400 containing 20 µl of the initial reaction, 8 µl PCR Buffer + MgCl2, 0.4 µM of standard Illumina
401 primers P5 and P7, and 80 µM dNTPs, and amplified a single cycle of 95°C for 1 minute, 60°C
402 for 2 min and 68°C for 5 min. Products were then purified and size-selected using NucleoMag
403 beads (Macherey-Nagel, Düren, Germany) for two rounds of purification/size selection according
404 to the supplied protocol at a ratio of bead solution 1.3 times the reaction volume and eluted in 30

405 μ l EBT. Purified libraries were quantified using a Nanodrop ND-1000 spectrophotometer (Thermo
406 Fisher Scientific, Waltham, Massachusetts, USA), Bioanalyzer2100 (Agilent, Santa Clara,
407 California, USA), Qubit 2.0 Fluorometer (Thermo Fisher Scientific), and qPCR reaction. 46 to 148
408 ng of DNA were enriched for human mitochondrial sequence in two rounds of capture using 1200
409 ng of biotinylated RNA baits reverse transcribed from human mitochondrial PCR products
410 (courtesy of L. Cardin and S. Brunel.) following the protocol described in Massilani *et al.*⁴⁵, but
411 with four changes: (1) for hybridization and wash steps, 60°C was used instead of 62°C. (2)
412 DNA/RNA-bait solution was incubated 96 H instead of 48 H. (3) Elution of the bead-bound
413 enriched DNA was performed with a 5 minute incubation in 30 μ l EBT at 95°C followed by a
414 magnetic bead separation and the transfer of the eluate to a new tube rather than a 0.1 N NaOH
415 elution followed by silica column purification. (4) All post-capture amplifications were performed
416 for 35 cycles followed by a heteroduplex resolution step as described above. Enriched DNA was
417 then quantified as above, and products from all libraries were pooled in equimolar amounts and
418 sequenced on an Illumina MiSeq using a v3 reagent kit for 2x76 cycles, substituting primer CL72
419 for the Read1 sequencing primer as described⁴⁴.

420 Eight additional libraries along with positive and negative controls were made from 3-8 μ l each of
421 the remaining extract BK_A4B, which had the highest relative endogenous DNA content. It should
422 be noted that this extract was derived from the portion of the cranial fragment which included the
423 suture. Libraries were prepared as described above except one library was first treated with USER
424 enzyme (New England Biolabs, Ipswich, Massachusetts, USA) for 30 min to remove deaminated
425 cytosine damage. Prior to the barcoding amplification, a 6-cycle amplification of pre-barcoded
426 libraries was performed using 45 μ l of each library with 45 μ l OneTaq 2X Master Mix with
427 Standard Buffer (New England Biolabs), and 0.1 μ M internal primers CL72⁴⁴ and CL130⁴⁰ with

428 the above PCR conditions. Three pairs of different dual-barcoded adapters were then used to
429 amplify 20 µl of each amplified library, followed by purification and size selection as described
430 above, which allowed the later pooling of two enrichment protocols and non-enriched DNA from
431 the same library. An average of 1.2 µg of DNA to 1 µg RNA-baits was used for each mitochondrial
432 enrichment, as above, however, an additional alternative “touch-down” hybridization protocol
433 consisting of 60°C for 12 H, 59°C for 12 H, 58°C for 12 H, 57°C for 12 H, and 56°C for 48 H was
434 tested for each library. For select libraries, an alternative wash protocol described in Fu *et al.*⁴⁶ was
435 also tested. Neither of these alternative protocols had a substantial impact on the results obtained.
436 Enriched and shotgun libraries were then pooled separately and size selected on an E-Gel
437 SizeSelect 2% agarose gel (Thermo Fisher). Enriched libraries were then sequenced on an Illumina
438 MiSeq, as above, and shotgun libraries were sequenced on an Illumina NextSeq using a NextSeq
439 500/550 High Output Kit v2 (2x75 cycles).

440 **Data analysis**

441 Paired-end sequencing results were merged and adapters trimmed using leeHom⁴⁷, and reads were
442 then aligned to the human genome (hg37d5) with BWA (v0.7.12) aln, parameters -n 0.01 -l 0,
443 followed by samse⁴⁸. Reads shorter than 28 bp long were then removed directly from sam files
444 with an awk command³⁹. PCR duplicates were removed using MarkDuplicates (v2.9.0)⁴⁹ and reads
445 mapping with quality less than 25 were removed with SAMtools (v1.7)⁵⁰. Reads mapping to the
446 nuclear genome with a mapping quality score of 25 or greater were locally realigned around known
447 indels using GATK (v3.7-0) IndelRealigner⁵¹. Following this step, mapped reads less than 35 bp
448 containing indels were removed⁵². This step reduced aberrant SNP calls due to spurious alignments
449 of short fragments in our dataset, where the base did not match either of two expected alleles, from
450 1.1% to 0.6%. In comparison, raising the minimum length of all reads to 30 bp reduced aberrant

451 SNP calls to 0.4%, but reduced informative SNPs by 18.4%, demonstrating the utility of retaining
452 a short minimum read length while excluding short indel-containing reads for this sample. All
453 libraries showed extremely poor preservation of genetic material. The average fragment length of
454 mapped reads after the above treatment was 38 bp, and the first position C>T transition rate from
455 damage was 55% at the 5' end of the molecule as calculated by mapDamage (v2.0.6)⁵³ (Extended
456 Data Figure 12).

457 Reads mapping to the mitochondrion were used to determine the posterior probability for
458 contaminating modern human sequences with Schmutzi⁵⁴ and found to have a distribution
459 maximum at 1%. A mitochondrial consensus sequence was called from the majority of bases at
460 each position using Geneious (v8.1.9)⁵⁵, which exactly matched that generated from Schmutzi.
461 The 5'-most 100 bp of this consensus sequence was duplicated at the 3' end and used as a reference
462 for a new alignment using the enriched reads. The haplogroup was called using Phy-Mer with
463 Build 16 rCRS-based haplogroup motifs⁵⁶ and verified by manual analysis of sequence changes.
464 A Bayesian tree of 25 ancient and 3 modern mitochondrial sequences, excluding the hypervariable
465 regions, was constructed using MrBayes⁵⁷ using a GTR+i+G nucleotide substitution model, which
466 gave the lowest log-likelihood for the tree out of all models tested (GTR and HKY with all
467 combinations of 4 invariant sites and gamma distributions), agreeing with the results of
468 JModelTest2⁵⁸. The chain was run for 1,100,000 iterations, subsampled every 200 after discarding
469 a 9% burn-in period and visualized using FigTree v. 1.4.3
470 (<http://tree.bio.ed.ac.uk/software/figtree>). A list of sources for the mitochondrial sequences is
471 given in Table S5.

472 Genetic sex was determined using the ratio of sequences aligning to the X and Y chromosomes,
473 given as the R_y value, as described in Skoglund, *et al.*²⁶. An additional calculation of the ploidy of

474 the X chromosome using read counts mapping to the X chromosome to the autosomes,
475 ($Reads_X/Reads_{\text{autosomes}}$) was also performed. SNPs informative for the Y-chromosome haplogroup
476 were identified using Yleaf (v1.0)⁵⁹ for reads with mapping quality scores of both 10 and 20
477 (Supplementary Data 1).

478 **Neanderthal content**

479 Neanderthal ancestry was calculated using the ancestry informative SNP method¹ calculated
480 separately for Neanderthal- or AMH-derived SNPs on four libraries prepared from two
481 independent extractions, treated either with or without UDG. The combined libraries overlapped
482 a total of 6,252 SNPs reported to have derived in either the Neanderthal (2,538 SNPs) or AMH
483 (3,714 SNPs) lineages⁶⁰. The combined libraries averaged 3.5% (SD 0.0074) Neanderthal
484 ancestry. To test the sensitivity of these SNPs to determine Neanderthal ancestry, this SNP subset
485 was then used to recalculate Neanderthal ancestry from several previously reported UP genomes¹.
486 The results agreed with previously reported values (Table S4).

487 **SNP calling and f-statistics**

488 BuranKaya3A bam files for all barcoded libraries were merged with SAMtools merge⁵⁰ and PCR
489 duplicates removed with MarkDuplicates⁴⁹. SNPs were called for positions overlapping with the
490 combined SNP panels from Fu *et al.*¹ using SAMtools mpileup⁵⁰, requiring a SNP base quality
491 score of 30 or greater, and choosing one allele at random when necessary with pileupcaller⁶¹. This
492 resulted in 27,740 SNPs out of 2,990,848 being called for BuranKaya3A. To monitor the impact
493 cytosine deamination may have on the SNP calls and resulting analyses of ancient samples,
494 alternative datasets removing all C to T or G to A transitions were generated and all statistical
495 analyses were performed on both data sets. Results with >30% disagreement between the two
496 datasets were excluded from the analyses, but both datasets are included in the supplements.

497 To calculate f-statistics, data from 52 previously reported genomes (in either fastq or bam format)
498 were downloaded and realigned to the human genome (hg37d5), and SNPs were called following
499 the identical pipeline used for BuranKaya3A, with the exception that diploid SNP calls were
500 retained for high-coverage individuals used as an outgroup in f_3 analyses (list of samples and
501 references given in Table S6). Modern humans used in statistical analyses are from Mallick, et
502 al.⁶². “Mbuti” is a population of three modern Mbuti individuals. f_3 -statistics and D-statistics were
503 computed using ADMIXTOOLS²⁹ qp3Pop (v412) qpDstat (v712), respectively. Standard error
504 was estimated using a block jackknife with 0.050 centiMorgan blocks. Full analyses performed
505 and results for $f_3(x, y; \text{Mbuti})$ and $D(w, y; \text{BuranKaya3, Mbuti})$ are given in Table S7 and
506 Supplementary Data 2, respectively.

507 **Data Availability**

508 Sequence data generated in this study will be made available upon publication.

509 **References**

- 510 1. Fu, Q. *et al.* The genetic history of Ice Age Europe. *Nature* **534**, 200–205 (2016).
- 511 2. Prat, S. *et al.* The Oldest Anatomically Modern Humans from Far Southeast Europe: Direct
512 Dating, Culture and Behavior. *PLoS ONE* **6**, e20834 (2011).
- 513 3. Noiret, P. De quoi Gravettien est-il le nom ? in *Les Gravettians* 29–64 (Paris: Editions Errance,
514 2013).
- 515 4. Kozlowski, J. K. The origin of the Gravettian. *Quat. Int.* **359–360**, 3–18 (2015).
- 516 5. Conard, N. J. & Moreau, L. Current Research on the Gravettian of the Swabian Jura.
517 *Mitteilungen Ges. Für Urgesch.* **13**, 29–59 (2004).
- 518 6. Karel Valoch. L’origine du Gravettien de l’Europe centrale. in *The Upper Palaeolithic (ed*
519 *Palma Di Cesnola, A., Montet-White, A. & Valoch, K.)* **6**, 203–211 (1996).

520 7. Svoboda, J. A. On Modern Human Penetration to Northern Eurasia: the Multiple Advances
521 Hypothesis. in *Rethinking the human revolution : new behavioural and biological perspectives*
522 *on the origin and dispersal of modern humans* **19**, 329–339 (McDonald Institute for
523 Archaeological Research, Cambridge, UK : Oxford, UK ; Oakville, 2007).
524 8. Hoffecker, J. F. & Holliday, V. T. Landscape Archaeology and the Dispersal of Modern
525 Humans in Eastern Europe. in *The Upper Paleolithic of Northern Eurasia and America: Sites,*
526 *Cultures, Traditions* 140–158 (Petersburg 2014).
527 9. Golovanova, L. V. & Doronichev, V. B. VII - The Early Upper Paleolithic of the Caucasus in
528 the West Eurasian Context. in *The Aurignacian of Yafteh Cave and its context (2005-2008*
529 *excavations)* 137–160 (Liège University, 2012).
530 10. Bar-Yosef, O. *et al.* Dzudzuana: an Upper Palaeolithic cave site in the Caucasus foothills
531 (Georgia). *Antiquity* **85**, 331–349 (2011).
532 11. Golovanova, L. V. *et al.* The Early Upper Paleolithic in the northern Caucasus (new data
533 from Mezmaiskaya Cave, 1997 excavation). *Eurasian Prehistory* **4**, 43–78 (2012).
534 12. Hoffecker, J. F. The early upper Paleolithic of eastern Europe reconsidered. *Evol.*
535 *Anthropol. Issues News Rev.* **20**, 24–39 (2011).
536 13. Hublin, J.-J. The modern human colonization of western Eurasia: when and where? *Quat.*
537 *Sci. Rev.* **118**, 194–210 (2015).
538 14. Demidenko, Y. E. Crimean Upper Paleolithic. in *Encyclopedia of Global Archaeology* (ed.
539 Smith, C.) 1782–1791 (Springer New York, 2014). doi:10.1007/978-1-4419-0465-2_1864
540 15. Bar-Yosef, O., Belfer-Cohen, A. & Adler, D. S. The Implications of the Middle-Upper
541 Paleolithic Chronological Boundary in the Caucasus to Eurasian Prehistory. *Anthropologie*
542 **XLIV**, 49–60 (2006).

543 16. Hoffecker, J. F. A New Framework for the Upper Paleolithic of Eastern Europe. (2012).

544 17. Svoboda, J. A. The Gravettian on the Middle Danube. *PALEO Rev. Archéologie*
545 *Préhistorique* **19**, 203–220 (2007).

546 18. Lazaridis, I. *et al.* Paleolithic DNA from the Caucasus reveals core of West Eurasian
547 ancestry. Preprint at bioRxiv doi: <https://doi.org/10.1101/423079>.

548 19. Péan, S., Puaud, S., Crépin, L., Prat, S. & Quiles, A. The Middle to Upper Paleolithic
549 Sequence of Buran-Kaya III (Crimea, Ukraine): New Stratigraphic, Paleoenvironmental, and
550 Chronological Results. *Radiocarbon* **55**, 1454–1469 (2013).

551 20. Yanevich, A. Les occupations gravettiennes de Buran-Kaya III (Crimée): contexte
552 archéologique. *L'Anthropologie* **118**, 554–566 (2014).

553 21. Fu, Q. *et al.* An early modern human from Romania with a recent Neanderthal ancestor.
554 *Nature* **524**, 216–219 (2015).

555 22. Fernandes, V. *et al.* The Arabian Cradle: Mitochondrial Relicts of the First Steps along the
556 Southern Route out of Africa. *Am. J. Hum. Genet.* **90**, 347–355 (2012).

557 23. Costa, M. D. *et al.* A substantial prehistoric European ancestry amongst Ashkenazi
558 maternal lineages. *Nat. Commun.* **4**, (2013).

559 24. Haak, W. *et al.* Ancient DNA from the First European Farmers in 7500-Year-Old Neolithic
560 Sites. *Science* **310**, 1016–1018 (2005).

561 25. Lazaridis, I. *et al.* Genomic insights into the origin of farming in the ancient Near East.
562 *Nature* **536**, 419–424 (2016).

563 26. Skoglund, P., Storå, J., Götherström, A. & Jakobsson, M. Accurate sex identification of
564 ancient human remains using DNA shotgun sequencing. *J. Archaeol. Sci.* **40**, 4477–4482
565 (2013).

566 27. Fitzsimmons, K. E., Hambach, U., Veres, D. & Iovita, R. The Campanian Ignimbrite
567 Eruption: New Data on Volcanic Ash Dispersal and Its Potential Impact on Human Evolution.
568 *PLoS ONE* **8**, e65839 (2013).

569 28. Higham, T. *et al.* The timing and spatiotemporal patterning of Neanderthal disappearance.
570 *Nature* **512**, 306–309 (2014).

571 29. Patterson, N. *et al.* Ancient Admixture in Human History. *Genetics* **192**, 1065–1093
572 (2012).

573 30. Bradley, B., Anikovich, M. & Engenii, G. Early Upper Paeolithic in the Russian Plain:
574 Streletskayan flaked stone artefacts and technology. *Antiquity* **69**, 989–998 (1995).

575 31. Dobrovolskaya, M., Richards, M.-P. & Trinkaus, E. Direct radiocarbon dates for the Mid
576 Upper Paleolithic (eastern Gravettian) burials from Sunghir, Russia. *Bull. Mém. Société
577 Anthropol. Paris* **24**, 96–102 (2012).

578 32. Pettitt, P. B. & Bader, N. O. Direct AMS radiocarbon dates for the Sungir mid Upper
579 Palaeolithic burials. *Antiquity* **74**, 269–270 (2000).

580 33. Posth, C. *et al.* Pleistocene Mitochondrial Genomes Suggest a Single Major Dispersal of
581 Non-Africans and a Late Glacial Population Turnover in Europe. *Curr. Biol.* **26**, 827–833
582 (2016).

583 34. Lipson, M. & Reich, D. A working model of the deep relationships of diverse modern
584 human genetic lineages outside of Africa. *Mol. Biol. Evol.* **34**, 889–902 (2017).

585 35. Sintysyn, A. A. Les Sepultures de Kostenki: Chronologie, Attribution Culturelle, Rite
586 Funéraire. in *La Spiritualité, Actes du colloque de la commission 8 de l'UISPP (Paléolithique
587 supérieur), Liège, 10-12 décembre 2003*. 237–244 (Etudes et Recherches Archeologiques de
588 l'Universite de Liege, 2004).

589 36. Sikora, M. *et al.* Ancient genomes show social and reproductive behavior of early Upper
590 Paleolithic foragers. *Science* **358**, 659–662 (2017).

591 37. Jones, E. R. *et al.* Upper Palaeolithic genomes reveal deep roots of modern Eurasians. *Nat.*
592 *Commun.* **6**, (2015).

593 38. Reimer, P. J. *et al.* INTCAL13 and MARINE13 radiocarbon age calibration curves 0–
594 50,000 years CAL BP. *Radiocarbon* **55**, 1869–1887 (2013).

595 39. Bennett, E. A. *et al.* Library construction for ancient genomics: single strand or double
596 strand? *BioTechniques* **56**, 289–298 (2014).

597 40. Korlević, P. *et al.* Reducing microbial and human contamination in DNA extractions from
598 ancient bones and teeth. *BioTechniques* **59**, (2015).

599 41. Gorgé, O. *et al.* Analysis of Ancient DNA in Microbial Ecology. *Methods Mol. Biol.*
600 *Clifton NJ* **1399**, 289–315 (2016).

601 42. Glocke, I. & Meyer, M. Extending the spectrum of DNA sequences retrieved from ancient
602 bones and teeth. *Genome Res.* **27**, 1230–1237 (2017).

603 43. Gansauge, M.-T. *et al.* Single-stranded DNA library preparation from highly degraded
604 DNA using T4 DNA ligase. *Nucleic Acids Res.* **45**, e79 (2017).

605 44. Gansauge, M. T. & Meyer, M. Single-stranded DNA library preparation for the sequencing
606 of ancient or damaged DNA. *Nat Protoc* **8**, 737–48 (2013).

607 45. Massilani, D. *et al.* Past climate changes, population dynamics and the origin of Bison in
608 Europe. *BMC Biol.* **14**, 93 (2016).

609 46. Fu, Q. *et al.* DNA analysis of an early modern human from Tianyuan Cave, China. *Proc.*
610 *Natl. Acad. Sci.* **110**, 2223–2227 (2013).

611 47. Renaud, G., Stenzel, U. & Kelso, J. leeHom: adaptor trimming and merging for Illumina
612 sequencing reads. *Nucleic Acids Res.* **42**, e141–e141 (2014).

613 48. Li, H. & Durbin, R. Fast and accurate short read alignment with Burrows-Wheeler
614 transform. *Bioinformatics* **25**, 1754–60 (2009).

615 49. <http://broadinstitute.github.io/picard/>.

616 50. Li, H. *et al.* The Sequence Alignment/Map format and SAMtools. *Bioinformatics* **25**,
617 2078–9 (2009).

618 51. Van der Auwera, G. A. *et al.* From FastQ Data to High-Confidence Variant Calls: The
619 Genome Analysis Toolkit Best Practices Pipeline: The Genome Analysis Toolkit Best Practices
620 Pipeline. in *Current Protocols in Bioinformatics* 11.10.1-11.10.33 (John Wiley & Sons, Inc.,
621 2013).

622 52. de Filippo, C., Meyer, M. & Prüfer, K. Quantifying and reducing spurious alignments for
623 the analysis of ultra-short ancient DNA sequences. *BMC Biol.* **16**, (2018).

624 53. Jónsson, H., Ginolhac, A., Schubert, M., Johnson, P. L. F. & Orlando, L. mapDamage2.0:
625 fast approximate Bayesian estimates of ancient DNA damage parameters. *Bioinformatics* **29**,
626 1682–1684 (2013).

627 54. Renaud, G., Slon, V., Duggan, A. T. & Kelso, J. Schmutzi: estimation of contamination
628 and endogenous mitochondrial consensus calling for ancient DNA. *Genome Biol.* **16**, (2015).

629 55. Kearse, M. *et al.* Geneious Basic: an integrated and extendable desktop software platform
630 for the organization and analysis of sequence data. *Bioinformatics* **28**, 1647–9 (2012).

631 56. Navarro-Gomez, D. *et al.* Phy-Mer: a novel alignment-free and reference-independent
632 mitochondrial haplogroup classifier. *Bioinforma. Oxf. Engl.* **31**, 1310–1312 (2015).

633 57. Hulsenbeck, J. P. & Ronquist, F. MRBAYES: Bayesian inference of phylogenetic trees.
634 *Bioinformatics* **17**, 754–755 (2001).

635 58. Darriba, D., Taboada, G. L., Doallo, R. & Posada, D. jModelTest 2: more models, new
636 heuristics and parallel computing. *Nat. Methods* **9**, 772 (2012).

637 59. Ralf, A., Montiel González, D., Zhong, K. & Kayser, M. Yleaf: Software for Human Y-
638 Chromosomal Haplogroup Inference from Next-Generation Sequencing Data. *Mol. Biol. Evol.*
639 **35**, 1291–1294 (2018).

640 60. Prufer, K. *et al.* The complete genome sequence of a Neanderthal from the Altai
641 Mountains. *Nature* **505**, 43–49 (2014).

642 61. <https://github.com/stschiff/sequenceTools>.

643 62. Mallick, S. *et al.* The Simons Genome Diversity Project: 300 genomes from 142 diverse
644 populations. *Nature* **538**, 201–206 (2016).

645

646

647 **Acknowledgments**

648 We thank Olivier Gorgé for assistance with DNA sequencing. We thank also the National
649 Academy of Sciences of Ukraine for permission to excavate at Buran-Kaya III, and all the team
650 members of the 2001 and 2009–2011 excavation seasons. EAB was supported by the CNRS and
651 the Labex “Who am I”. SPr was supported by the Foundation Fyssen. SPe was supported by the
652 French National Research Agency (ANR-05-JCJC-0240-01). The field work was supported by the
653 Muséum National d’Histoire Naturelle (MNHN, Paris), the CNRS and French Ministry of Foreign
654 Affairs. The paleogenomic facility obtained support from the University Paris Diderot within the
655 program “Actions de recherches structurantes”. The sequencing facility of the Institut Jacques

656 Monod, Paris, was supported by grants from the University Paris Diderot, the Fondation pour la
657 Recherche Médicale (DGE2011123014), and the Région Ile-de-France (11015901).

658

659 **Author contributions**

660 EMG, SPr, and SP initiated the project, EMG and EAB designed the study. EAB performed the
661 laboratory work, EAB, TG, and EMG analysed the data, LC performed aseptic excavation of the
662 sample. SPr performed the anthropological analysis. AY, SP and SPu provided archaeological
663 data. EAB wrote the manuscript with input from EMG, TG, SPr, SP, LC, and AY.

664

665 **Competing Interests**

666 The authors declare that they have no competing interests that might have influenced the work
667 described in this manuscript.

668 Correspondence should be addressed to EAB (eabennett@gmail.com), TG
669 (thierry.grange@ijm.fr), or EMG (eva-maria.geigl@ijm.fr).

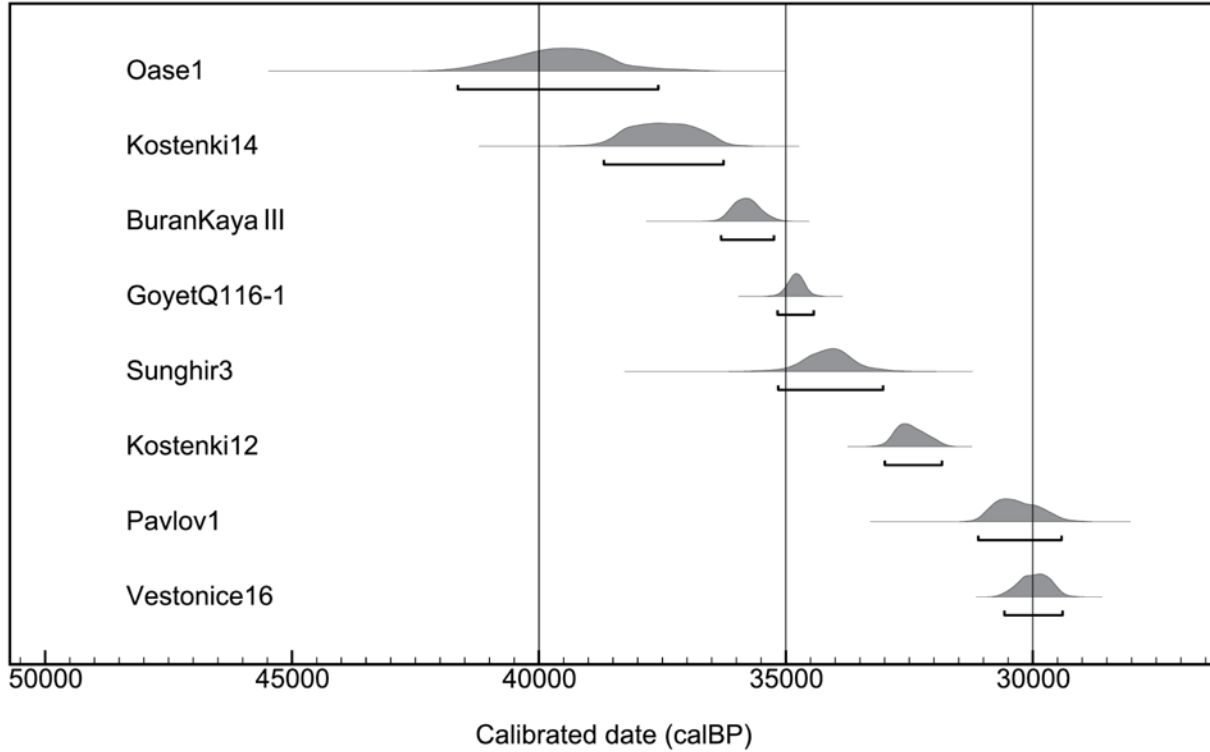
670

671

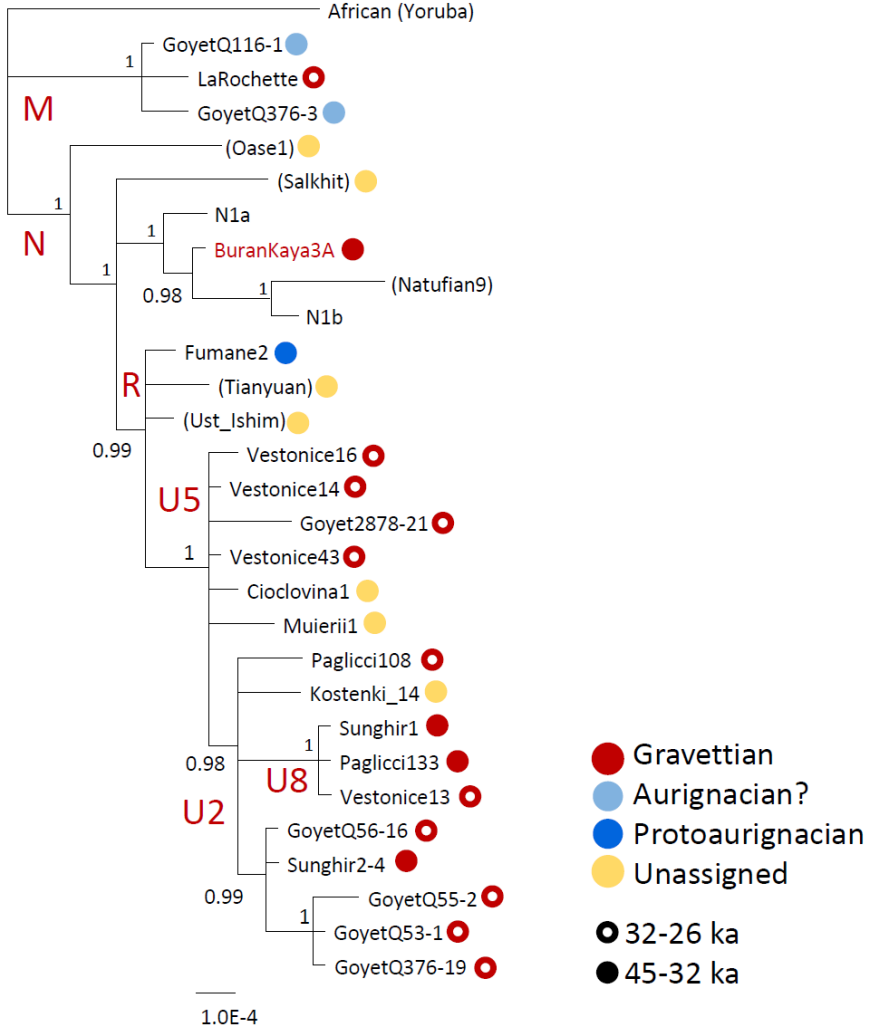
672

673

674

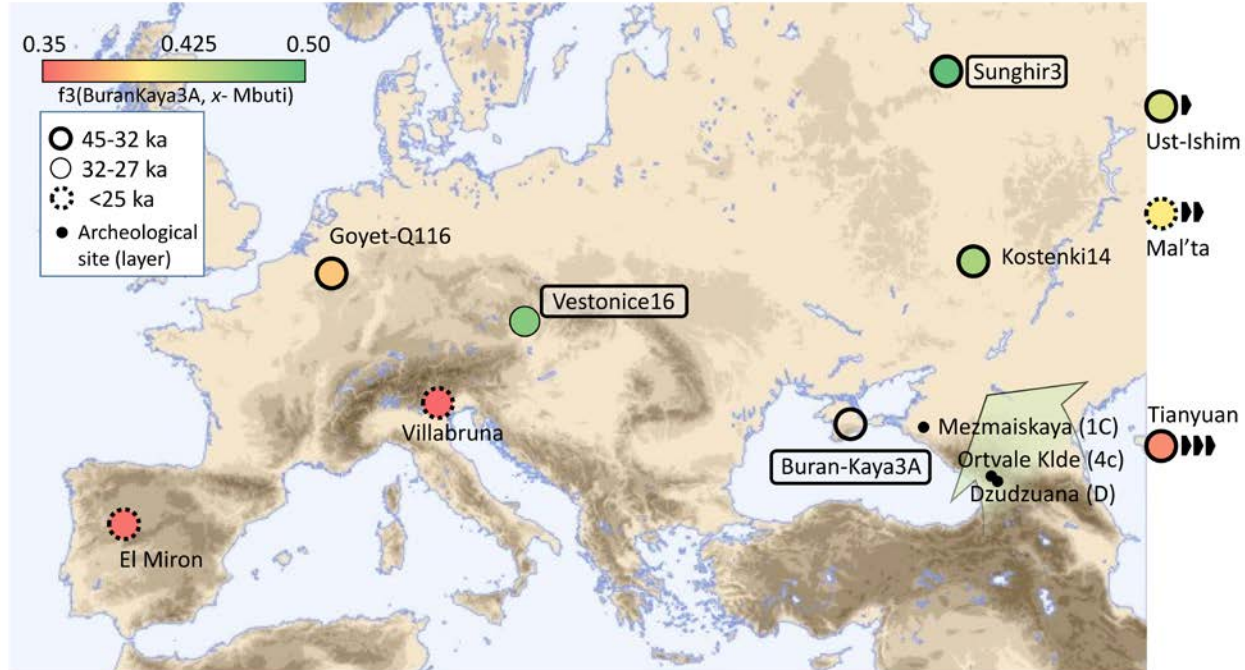


675 **Figure 1.** Recalibration of comparative AMS ^{14}C dates of Buran-Kaya III, layer 6-1 with Early
676 and Mid-Upper human Palaeolithic European samples. All dates were recalibrated using the
677 software OxCal v4.3.2 based on the IntCal13 calibration data set³⁸. For complementary
678 information on cultural contexts, see Table S1.



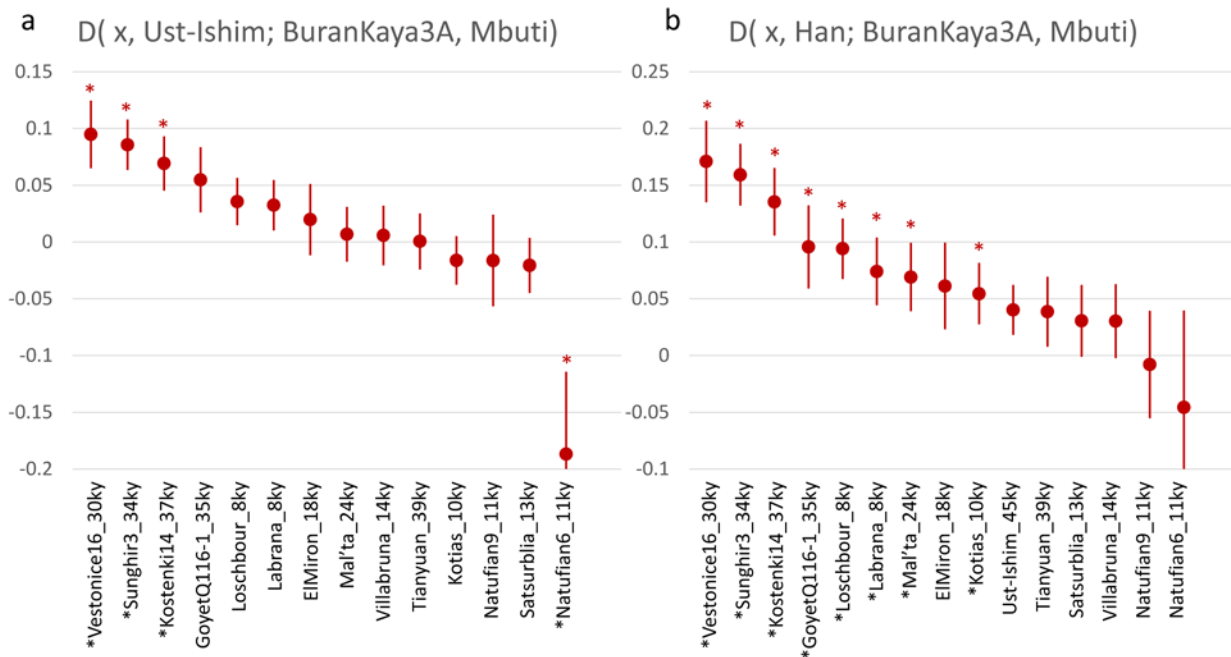
680

681 **Figure 2.** Bayesian phylogenetic tree of mitochondrial sequences, excluding Hyper-Variabile
682 Regions, from Early and Mid-Upper Palaeolithic individuals including BuranKaya3A. Posterior
683 probability indicated at the nodes. Non-European individuals are in parentheses. General ages
684 shown as either closed or open circles, and pre-glacial material cultures, when known, indicated
685 by colour. A question mark by the Aurignacian indicates a cultural assignment by dating rather
686 than direct association. Scale bar denotes substitutions per site. Sources for mitochondrial
687 sequences are listed in Table S5.



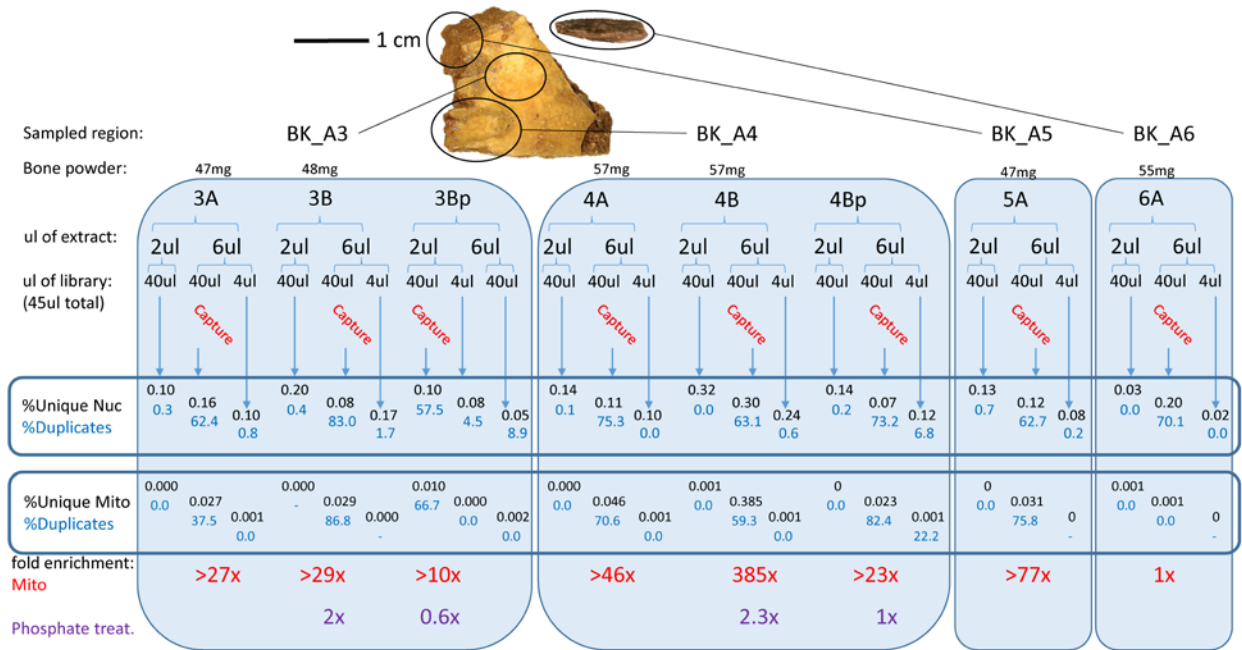
689 **Figure 3.** Location and heatmap of $f3(\text{BuranKaya3A}, x; \text{Mbuti})$ with archaeological sites
690 mentioned in the text. Values of high genomic coverage ancient samples (higher values show more
691 shared alleles with BuranKaya3A). Boxed text indicates samples associated with a Gravettian
692 archaeological context (including Sunghir3, alternatively described as Streletskian). Non-
693 European samples are given along the right margin at their approximate latitudes, their relative
694 distances indicated by black arrows. Archaeological sites for which no human genetic data are
695 available that contain micro-laminar industries comparable with Buran-Kaya III at
696 contemporaneous layers (in parentheses) indicated by black dots. A broad green arrow shows the
697 proposed EUP route introducing the Early Gravettian into Europe, suggested by the similar
698 features of these assemblages and the lack of a Common Western Eurasian genomic component
699 in BuranKaya3A.

700



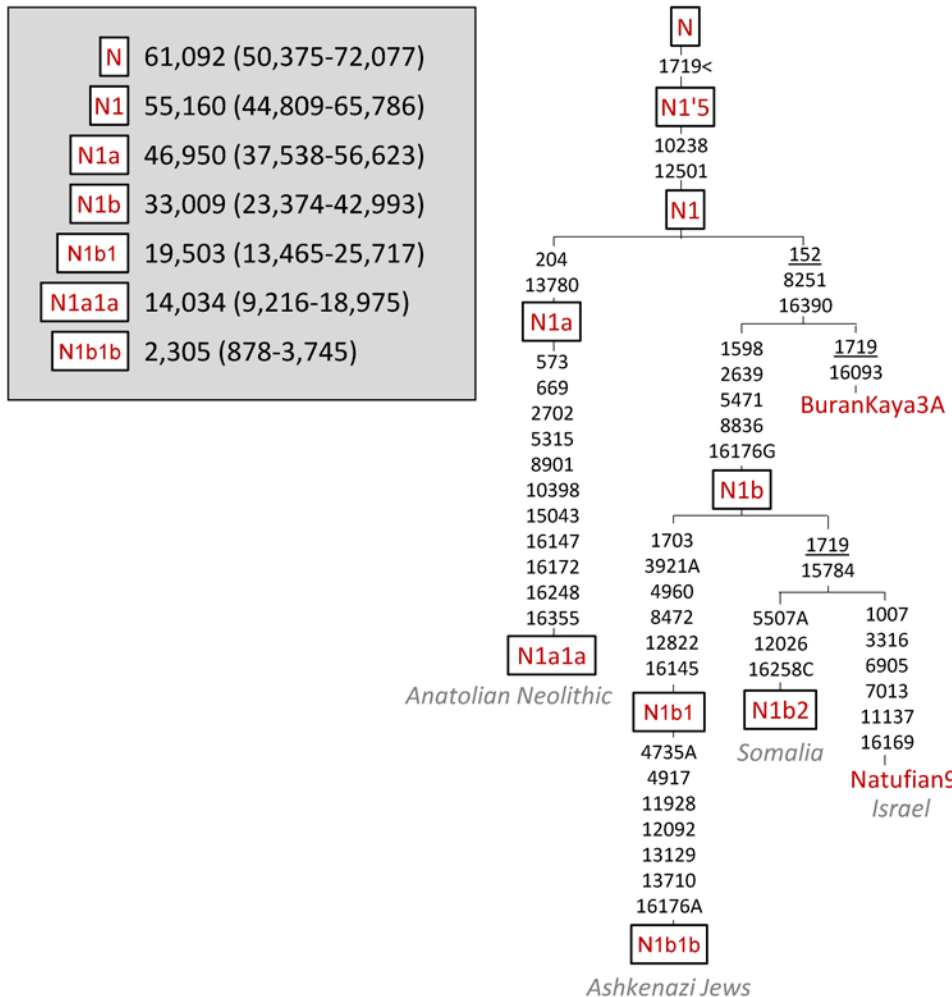
701

702 **Figure 4.** D-statistics results for a) $D(x, \text{Ust-Ishim}; \text{BuranKaya3A, Mbuti})$ and b) $D(x, \text{Han};$
703 $\text{BuranKaya3A, Mbuti})$ where $x = \text{selected UP and Mesolithic Eurasians}$. Starred individuals denote
704 a significant Z-score >2 . Approximate ages, being the mean of the latest calibrated published date
705 rounded to the nearest ky, are appended to the names. More positive values represent increased
706 allele sharing between x and *BuranKaya3A* relative to *Ust-Ishim* or *Han*, with *Mbuti* as an
707 outgroup. Results from all SNPs shown. All Z-scores and results from transversions only are given
708 in Extended Data Figure 4. The values for Kotias, Satsurblia, and the Natufians are distorted due
709 to Basal Eurasian content in these samples (see Extended Data Figure 9). Error bars = one standard
710 error.



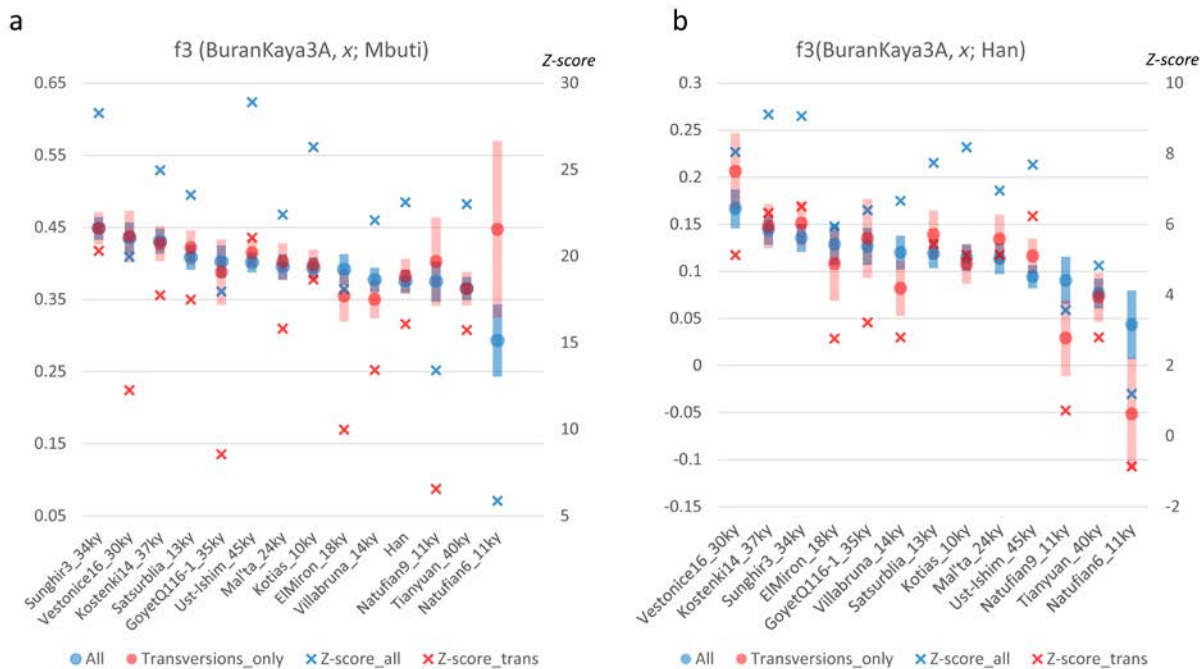
711

712 Extended Data Figure 1. Flowchart of screening methods and results of mitochondrial capture and
 713 phosphate enrichment for each library. Results show the percent of unique reads out of all reads
 714 28 nucleotides or greater mapping to the nuclear and mitochondrial references as well as the
 715 percent of PCR duplicates for each library. The suffix of sample numbers is as follows, A = no
 716 phosphate treatment, B = phosphate treated, Bp = phosphate treatment buffer. Extract BKA4B was
 717 selected for subsequent analysis. Original bone sample and regions used for each library is shown
 718 above. It has been noted that the region containing the darker suture yielded the best results.



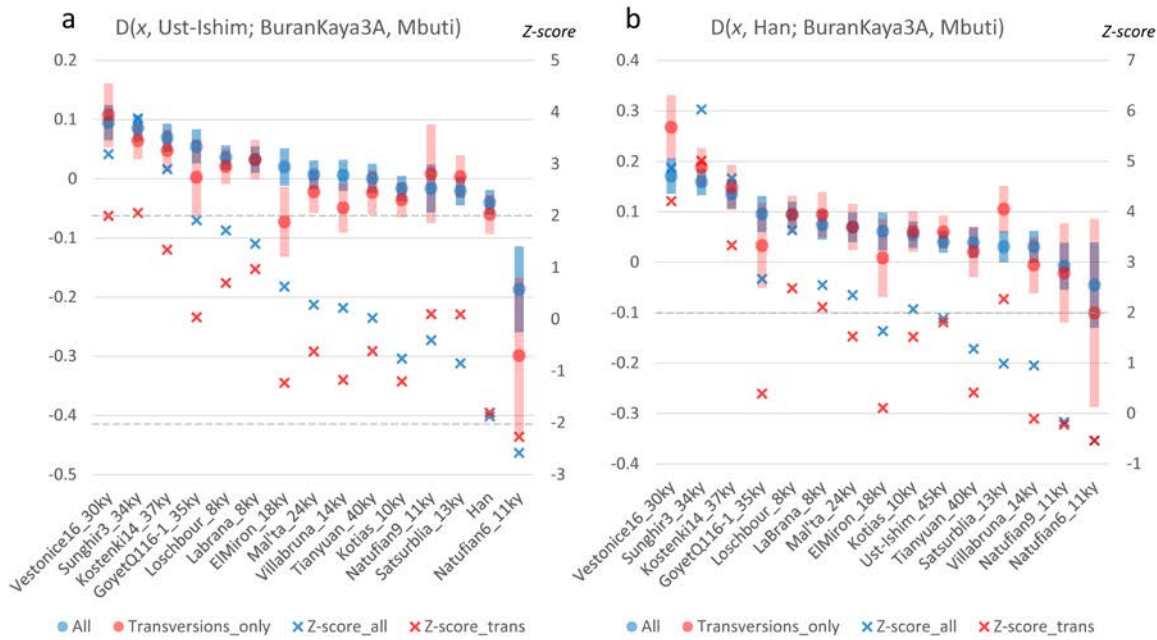
719

720 Extended Data Figure 2. Detailed mutation map of mitochondrial N clade with the positions of
 721 BuranKaya3A, the Epipalaeolithic Natufian (Natufian9), and lineages discussed in the text. Grey
 722 italics represent the population or geographical region where the clade is prominent. Inset indicates
 723 the maximum likelihood estimation of TMRCA values of the nodes with 95% CI from Fernandes
 724 et al.²². Mutation tree calculated by mtphyl version 5.003
 725 (<https://sites.google.com/site/mtphyl/home>) compared to the rCRS. Underlined positions represent
 726 back mutations.



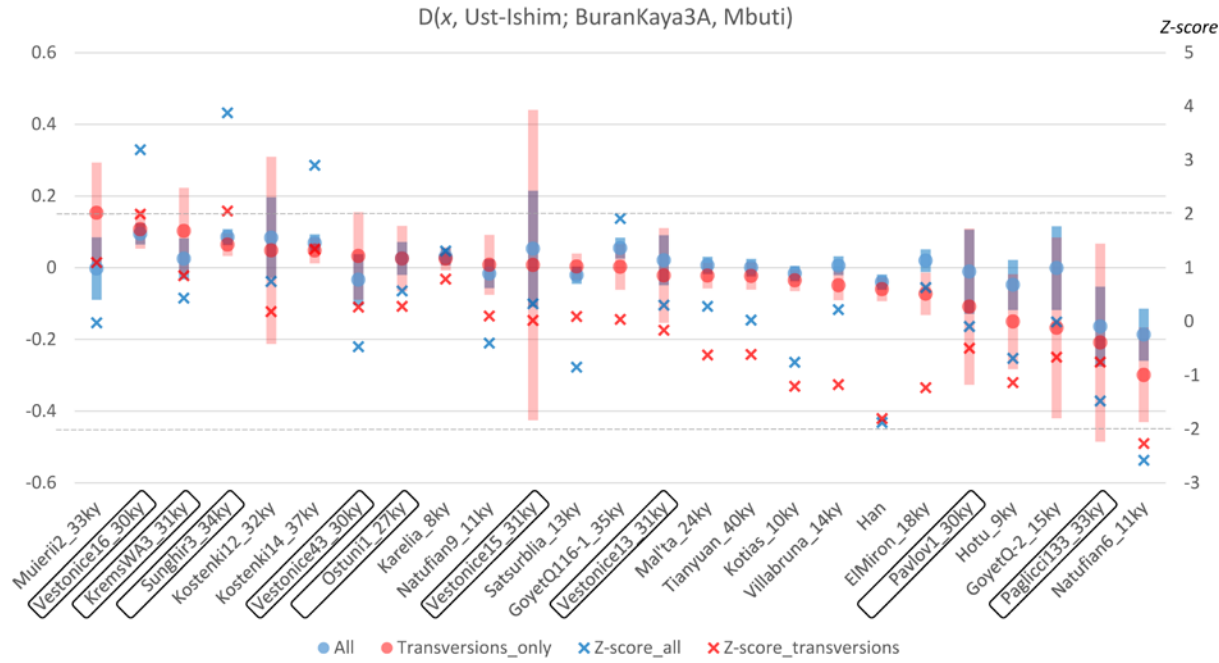
727

728 Extended Data Figure 3. Outgroup *f*3-statistics results showing the degree of shared alleles
 729 between BuranKaya3A and high-coverage UP Eurasians for outgroups Mbuti (a), Han (b). Left
 730 axis: *f*3-statistic corresponding to circles with error bars. Right axis: Z-score corresponding to “x”.
 731 Results for all SNPs are in blue, transversions only in red. The degree of overlap between blue and
 732 red shows the degree of agreement between the two datasets for a given sample combination.
 733 Approximate ages are appended to the names. Boxed names indicate individuals associated with
 734 a Gravettian context. Error bars = one standard error.



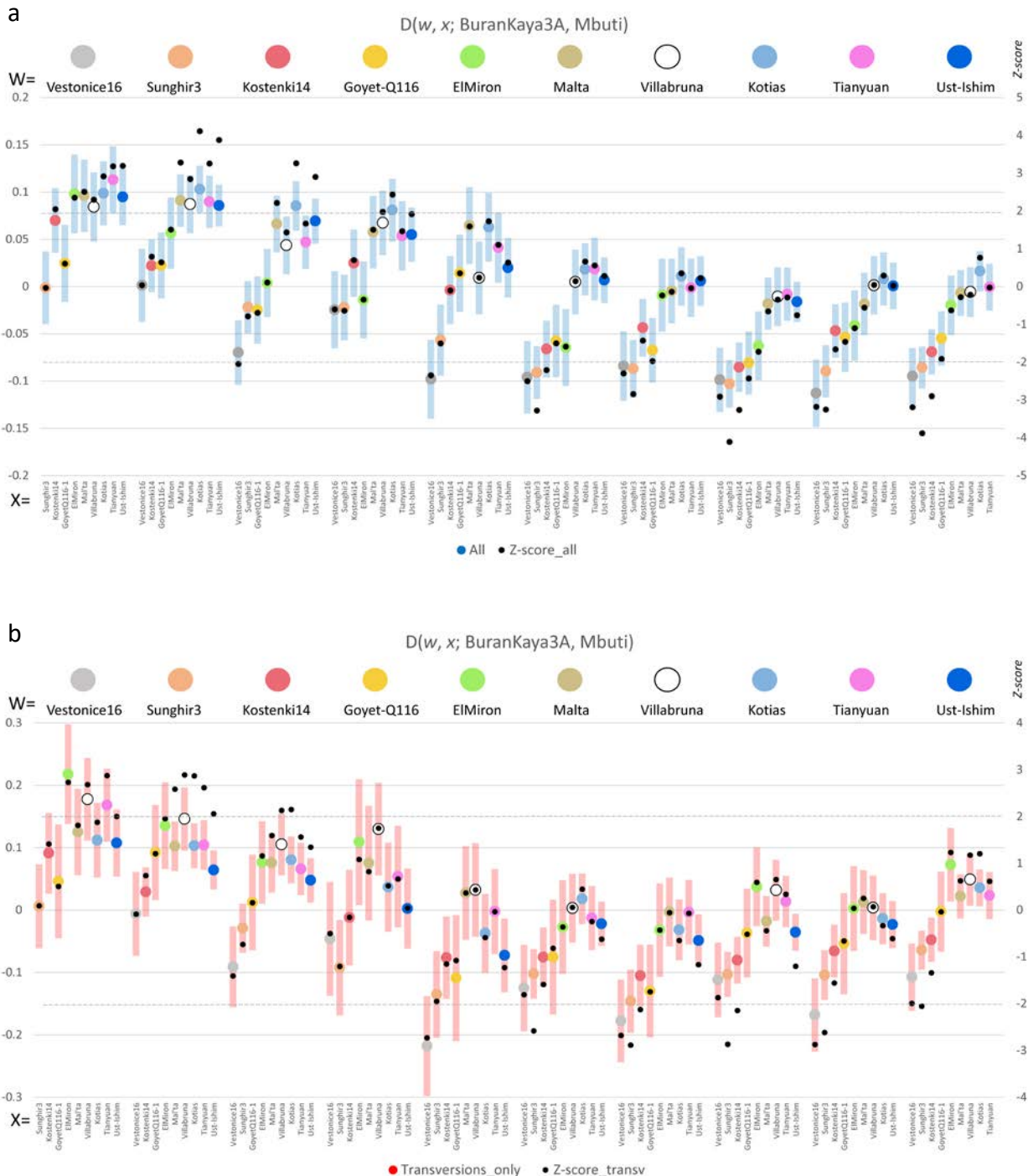
735

736 Extended Data Figure 4. D-statistics results for a) $D(x, \text{Ust-Ishim}; \text{BuranKaya3A}, \text{Mbuti})$ and b)
 737 $D(x, \text{Han}; \text{BuranKaya3A}, \text{Mbuti})$ where x = high coverage UP individuals. Left axis: D-statistic
 738 corresponding to circles with error bars. Right axis: Z-score corresponding to “x”. Results for all
 739 SNPs are in blue (shown also in Figure 4), transversions only in red. The degree of overlap between
 740 blue and red shows the degree of agreement between the two datasets for a given sample
 741 combination. Approximate ages are appended to the names. Boxed names indicate individuals
 742 associated with a Gravettian context. The values for Kotias, Satsurblia, and the Natufians are
 743 distorted in (a) due to Basal Eurasian content in these samples. Error bars = one standard error.



744

745 Extended Data Figure 5. D-statistics results for $D(x, \text{Ust-Ishim}; \text{BuranKaya3A, Mbuti})$ where $x =$
746 both high and low coverage UP individuals and a modern East Asian (Han). Only samples using
747 at least 100 transversion-only SNPs for the calculation are shown. Left axis: D-statistic
748 corresponding to circles with error bars. Right axis: Z-score corresponding to “x”. Results for all
749 SNPs are in blue, transversions only in red. The degree of overlap between blue and red shows the
750 degree of agreement between the two datasets for a given sample combination. Approximate ages
751 are appended to the names. Boxed names indicate individuals associated with a Gravettian context.
752 The values for Kotias, Satsurblia, and the Natufians are distorted due to Basal Eurasian content in
753 these samples. Error bars = one standard error.

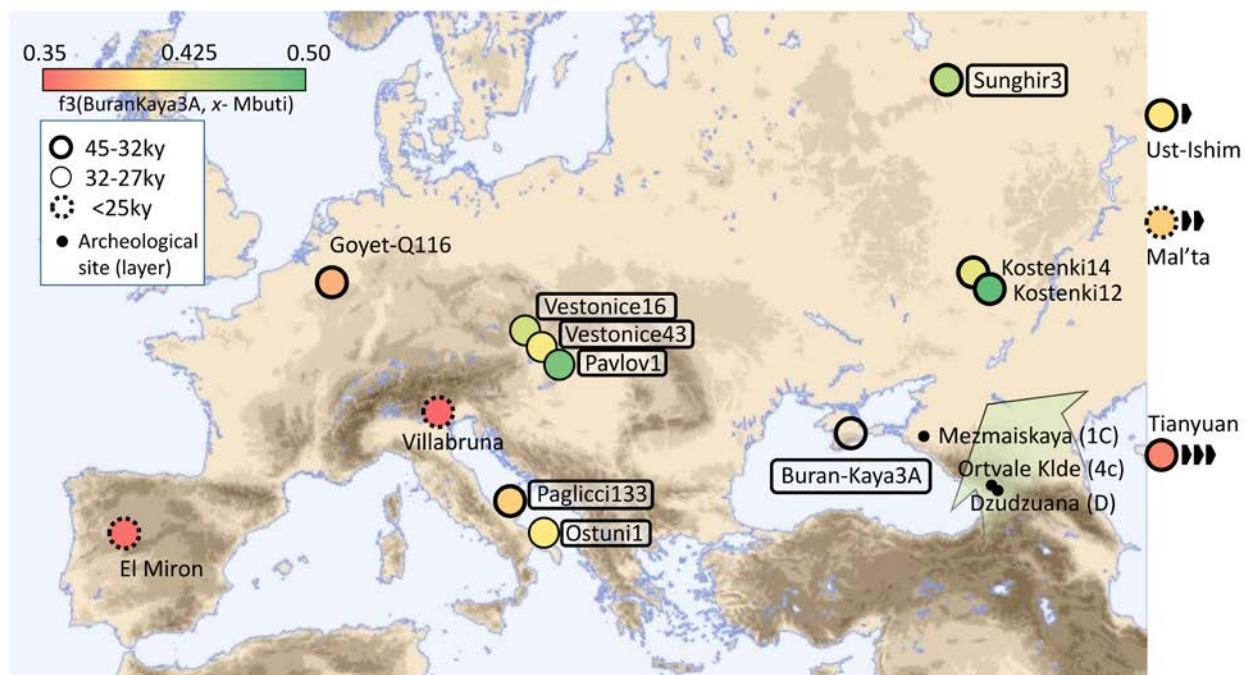


754

755

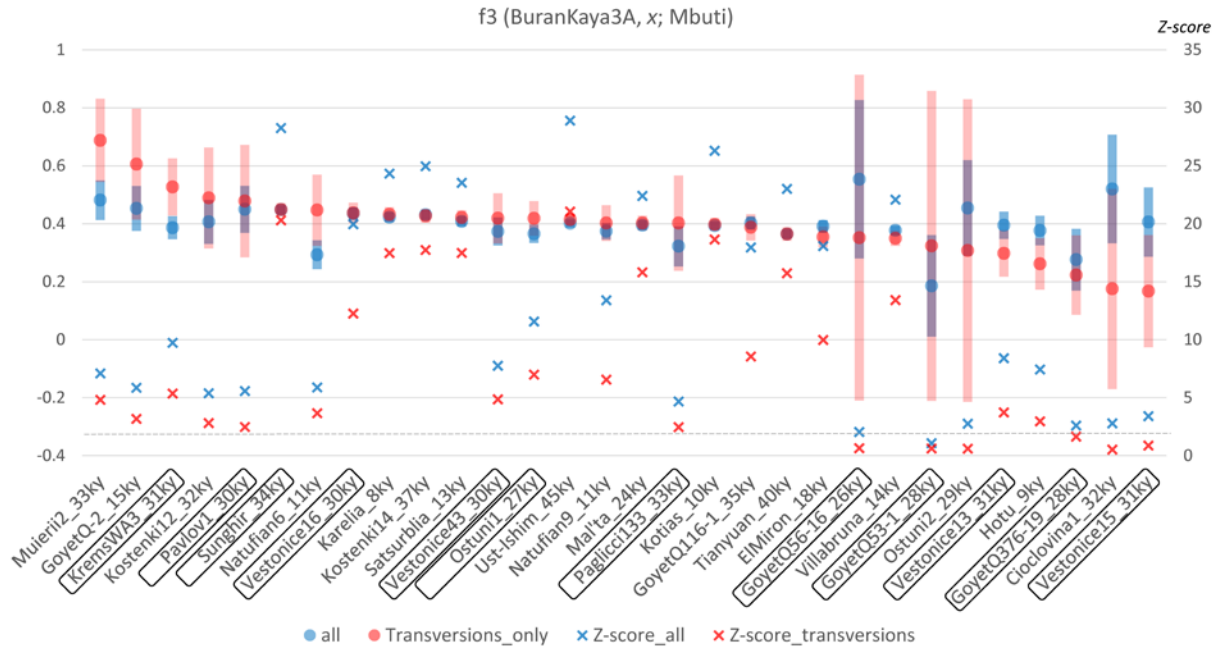
756 Extended Data Figure 6. D-statistics results for $D(w, x; \text{BuranKaya3A, Mbuti})$ where w and x are
 757 high-coverage UP Eurasians. More positive values show an excess of allele sharing of w over x
 758 with BuranKaya3A. Left axis: D-statistic corresponding to circles with error bars. Right axis: Z-

759 score corresponding to black dots. Significance (Z -score > 2) is indicated by horizontal dashed
760 lines. The values for Kotias are distorted due to Basal Eurasian content in this sample. Error bars
761 = one standard error. a) Results for all SNPs, b) results for transversions only.



762
763 Extended Data Figure 7. Location and heatmap of $f3$ (BuranKaya3A, x ; Mbuti) with archaeological
764 sites mentioned in the text. Values, as in Figure 3, but adding results from x including the lower-
765 coverage samples whose calculations made use of at least 50 transversion-only SNPs and were
766 within 30% agreement of values calculated using all SNPs. Boxed text indicates samples
767 associated with a Gravettian archaeological context (including Sunghir3, alternatively described
768 as Streletskian). Non-European samples are given along the right margin at their approximate
769 latitudes, their relative distances indicated by arrows. Archaeological sites for which no human
770 genetic data are available that contain micro-laminar industries comparable with Buran-Kaya III
771 at contemporaneous layers (in parentheses) indicated by black dots. A broad green arrow shows
772 the proposed EUP route introducing the Early Gravettian into Europe, suggested by the similar

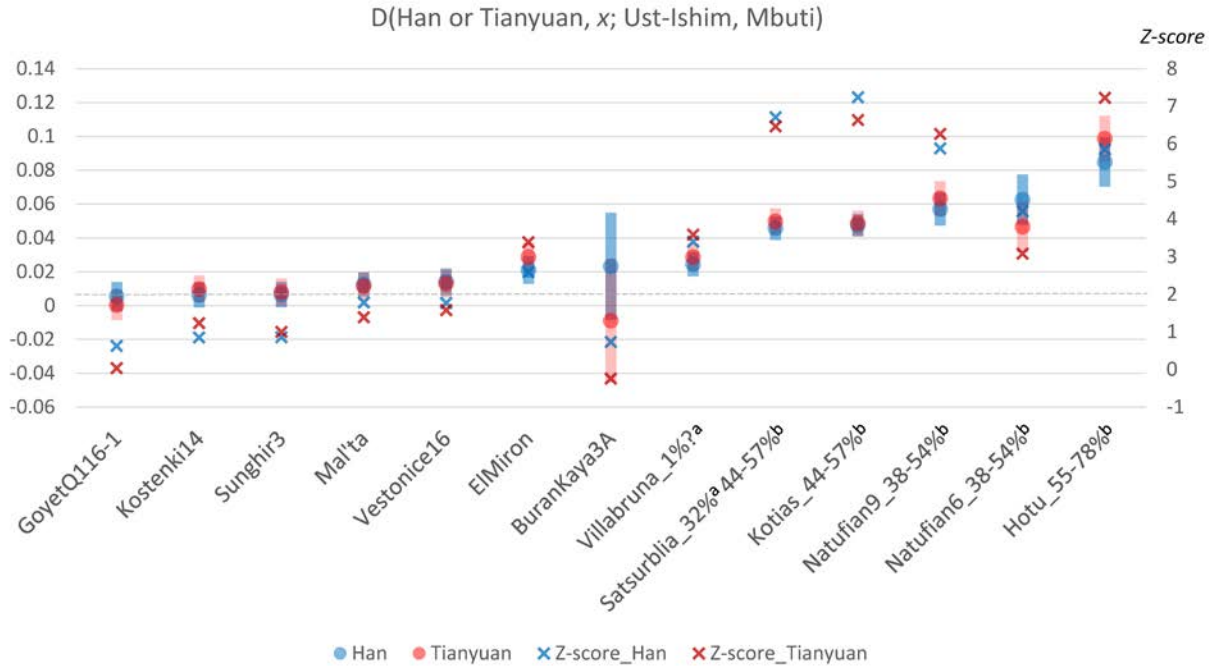
773 features of these assemblages and the lack of a Common Western Eurasian genomic component
774 in BuranKaya3A.



775

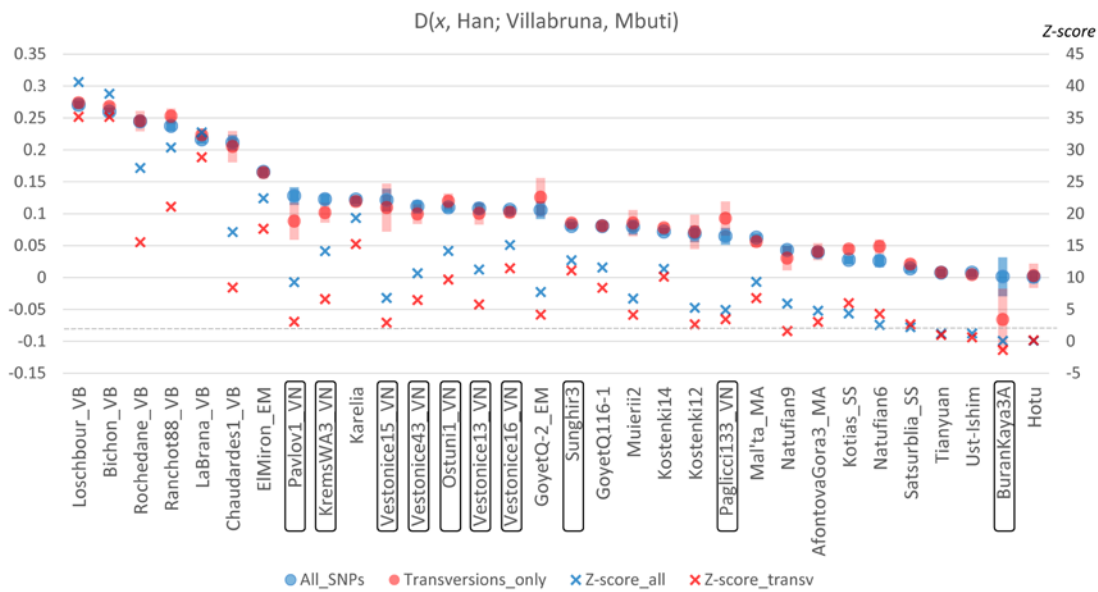
776 Extended Data Figure 8. Outgroup f_3 -statistics results showing the degree of shared alleles
777 between BuranKaya3A and UP Eurasians for outgroups Mbuti, $f_3(\text{BuranKaya3A}, x; \text{Mbuti})$, as in
778 Extended Data Figure 3A but including all samples for which values could be calculated. Left axis:
779 f_3 -statistic corresponding to circles with error bars. Right axis: Z-score corresponding to “x”.
780 Results for all SNPs are in blue, transversions only in red. The degree of overlap between blue and
781 red shows the degree of agreement between the two datasets for a given sample combination.
782 Approximate ages are appended to the names. Boxed names indicate individuals associated with
783 a Gravettian context. Error bars = one standard error.

784



785

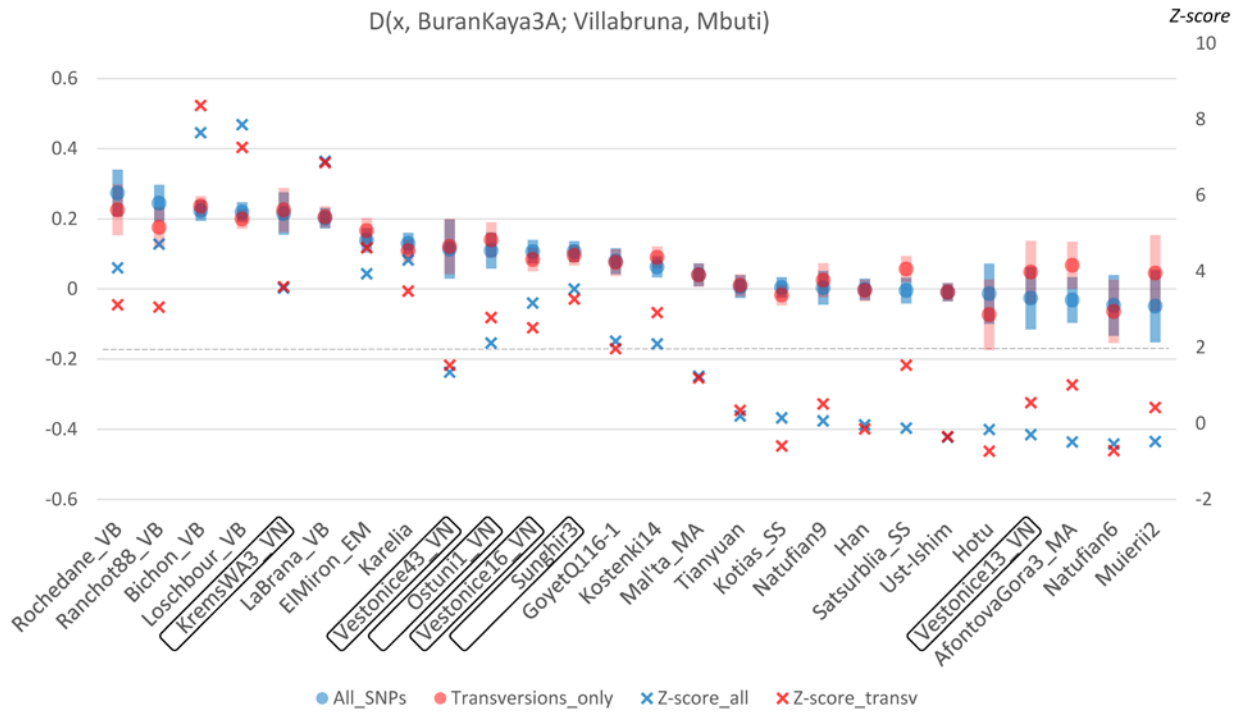
786 Extended Data Figure 9. Relative Basal Eurasian content as demonstrated by the statistic
787 $D(\text{Modern or Ancient East Asian}, x; \text{Ust-Ishim, Mbuti})^1$ using the transversions only SNP dataset.
788 Left axis: D-statistic corresponding to circles with error bars. Right axis: Z-score corresponding to
789 “x”. $x = \text{Han}$, blue, $x = \text{Tianyuan}$, red. Significance ($Z\text{-score} = 2$) is indicated by a horizontal dashed
790 line. Estimated Basal Eurasian content percentages given as suffixes to the names (a) estimated
791 from ADMIXTUREGRAPH¹, (b) one standard error range estimated from the f_4 ratio²⁵. Error
792 bars = one standard error.



793

794 Extended Data Figure 10. Relative Common West Eurasian content (as represented by Villabruna)
 795 given as $D(x, \text{Han}; \text{Villabruna, Mbuti})$ for ancient samples (x) using more than 1,000 SNPs for the
 796 calculation. More positive values signify an excess of shared alleles between x and Villabruna as
 797 compared to Han. Reported genetic clusters¹ given as suffixes to the names: VN, Vestonice; EM,
 798 ElMiron; VB, Villabruna; SS, Satsurblia; MA, Mal'ta. Boxed names indicate individuals
 799 associated with Gravettian contexts. Left axis: D-statistic corresponding to circles with error bars.
 800 Right axis: Z-score corresponding to “x”. Results for all SNPs are in blue, transversions only in
 801 red. The degree of overlap between blue and red shows the degree of agreement between the two
 802 datasets for a given sample combination. This value will be distorted for samples having Basal
 803 Eurasian content (see Extended Data Figure 9). Significance (Z-score = 2) is indicated by a
 804 horizontal dashed line. Error bars = one standard error.

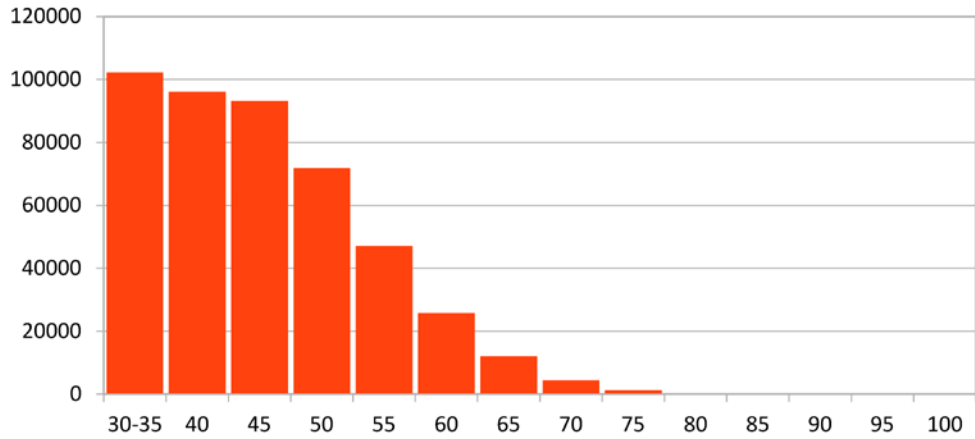
805



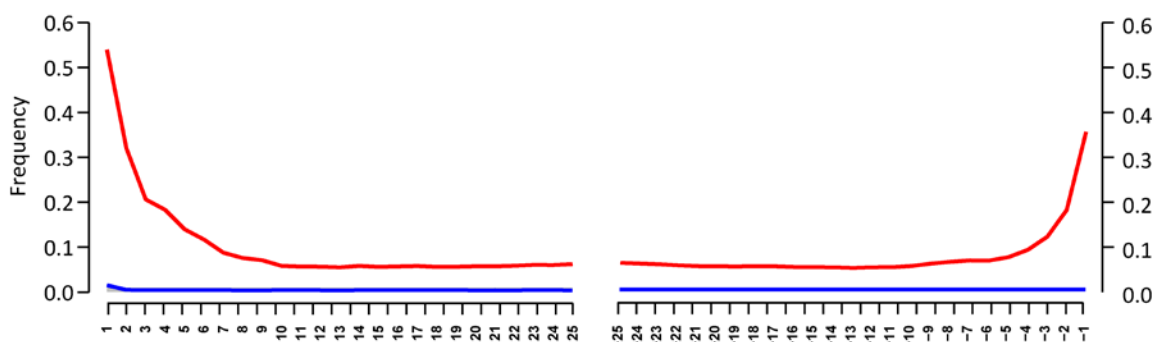
806

807 Extended Data Figure 11. Measuring the excess of shared alleles between Common West Eurasian
 808 (as represented by Villabruna) and x over BuranKaya3A using the D-statistic $D(x, \text{BuranKaya3A};$
 809 Villabruna, Mbuti). More positive values signify an excess of shared alleles between x and
 810 Villabruna compared to BuranKaya3A. Reported genetic clusters¹ given as suffixes to the names:
 811 VN, Vestonice; EM, ElMiron; VB, Villabruna; SS, Satsurblia; MA, Mal'ta. Boxed names indicate
 812 individuals associated with Gravettian contexts. Left axis: D-statistic corresponding to circles with
 813 error bars. Right axis: Z-score corresponding to “x”. Results for all SNPs are in blue, transversions
 814 only in red. The degree of overlap between blue and red shows the degree of agreement between
 815 the two datasets for a given sample combination. This value will be distorted for samples having
 816 Basal Eurasian content (Extended Data Figure 9). Significance (Z-score = 2) is indicated by a
 817 horizontal dashed line. Error bars = one standard error.

a



b



818

819 Extended Data Figure 12. a) Size distribution of recovered BuranKaya3A DNA fragments
820 mapping to the nuclear genome. b) The frequency of C to T mismatches due to cytosine
821 deamination of the first 25 nucleotides from the 5' and 3' ends of the DNA molecules. Graph
822 generated by mapDamage (v2.0.6)⁵³.